Acta Geologica Polonica, Vol. 74 (2024), No. 2, e9
DOI: 10.24425/agp.2024.150003

Spit bar deposits from the Upper Cretaceous (Cenomanian) transgressive sequence in NE Bohemia (Czechia)

ALINA CHRZĄSTEK[1] and JURAND WOJEWODA[2]

[1] *Institute of Geological Sciences, University of Wrocław, Maksa Borna 9, 50-204 Wrocław, Poland; e-mail: alina.chrzastek@uwr.edu.pl*
[2] *Faculty of Geoengineering, Mining and Geology, Wrocław University of Science and Technology, Na Grobli 15, 50-421 Wrocław, Poland; e-mail: jurand.wojewoda@pwr.edu.pl*

ABSTRACT:

Chrząstek, A. and Wojewoda, J. 2024. Spit bar deposits from the Upper Cretaceous (Cenomanian) transgressive sequence in NE Bohemia (Czechia). *Acta Geologica Polonica*, **74** (2), e9.

We propose a spit bar setting as the possible palaeoenvironment of the basal Late Cretaceous transgressive sequence in NW Bohemia. A new Cenomanian transgression model for the Bohemian Basin is also proposed. The uppermost Devět Křížů Sandstone, which has been conventionally referred to the Bohdašín Formation, probably represents the middle or lower upper Cenomanian (Upper Cretaceous), not the Triassic as previously supposed. We assume that this controversial unit was deposited before the main latest Cenomanian–early Turonian transgression. The spit bars were likely overgrown by vascular plants during their emergence in the late Cenomanian, and then inundated during the latest Cenomanian and early Turonian transgressive phases. The studied deposits had been intensively bioturbated, and the cf. *Taenidium* suite was recognized for the first time in them alongside the *Thalassinoides* assemblage (*T. paradoxicus*, *T. suevicus*, *Thalassinoides* isp., cf. *Thalassinoides*), which are characteristic of the *Scoyenia* and *Glossifungites* ichnofacies, respectively. The bioturbated, rhizolith-bearing horizon was presumably a paleosol.

Key words: Spit bar system; Ichnology; Rhizoliths; Cretaceous transgression; Palaeoenvironment; Palaeogeography; Geodynamic control.

INTRODUCTION

Spit bar systems are significant modern coastal features that are seldom recognized in the geological record (e.g., Merletti *et al*. 2018; Nehyba and Roetzel 2021). There are some difficulties in recognizing ancient spit bars, partly due to the lack of widely accepted depositional models describing their facies characteristics (see Johannessen and Nielsen 2009; Pancrazzi *et al*. 2022; Pellerin Le Bas *et al*. 2022 for discussion). They are documented mostly from the Quaternary (Nehyba and Roetzel 2021), with only a few examples known from older marine deposits: Upper Jurassic (Dreyer *et al*. 2005), Cretaceous (Merletti *et al*. 2018) and Palaeogene–Neogene (Rasmussen and Dybkjær 2005; Nehyba and Roetzel 2021).

Evans (1942, p. 846) defined a spit bar as "a ridge or embankment of sediment, attached to the land mass at one end and terminating in open water at the other. The crest of the spit from the land outward for some distance rises above the water." Nielsen and Johannessen (2009, p. 965) expanded Evans's (1942) definition by "the platform underlying the spit", which usually has a larger preservation potential that the subaerial spit (see also Meistrell 1972). A model of a complex recurved ('hacked') spit was postulated by King and Mc Cullagh (1971), as well as Ashton *et al*. (2007, p. 352), who suggested that spits also recurve or trend "back towards the shore, experiencing waves from a variety of directions."

Spit bar initiation and growth is mainly controlled by wave-induced longshore currents and cross-shore

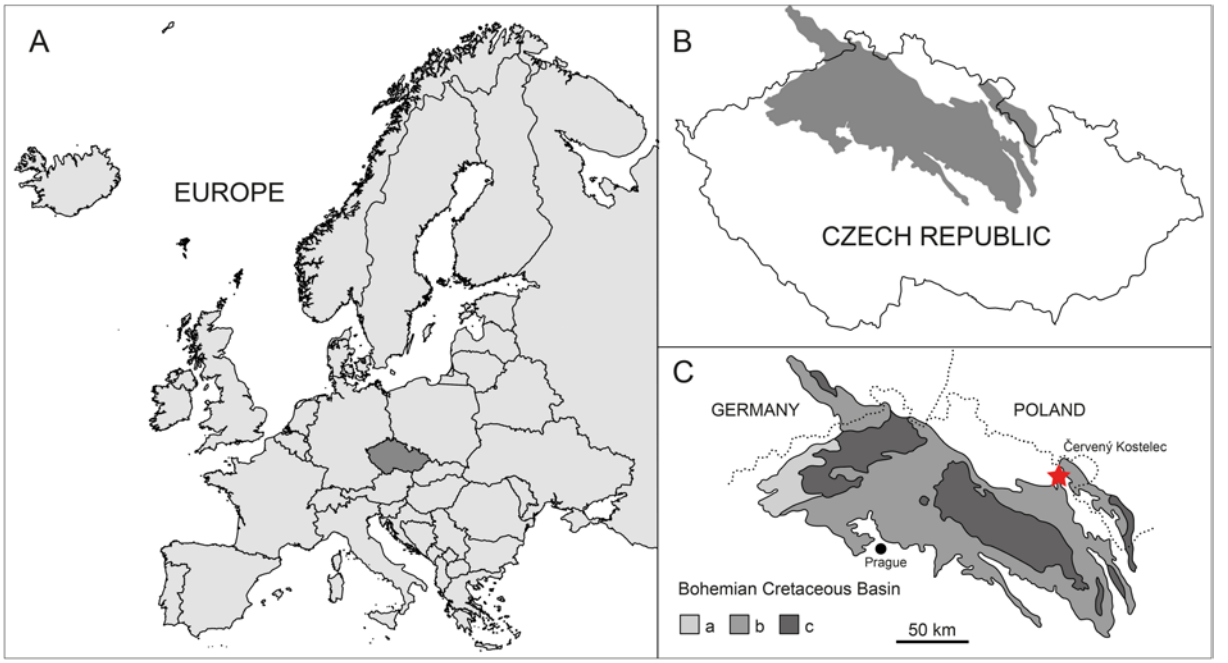

Text-fig. 1. Location of the study area; after Averianov and Ekrt (2015) and Fatka *et al*. (2022), slightly modified. A – Map of Europe showing the Czech Republic. B – Map of the Czech Republic with the location of the Bohemian Cretaceous Basin. C – Simplified geological map of the Bohemian Cretaceous Basin with detailed location of the Červený Kostelec area. Abbreviations: a – Cretaceous rocks covered by younger Palaeogene and Neogene deposits; b – Cenomanian to middle Turonian deposits; c – upper Turonian to Coniacian deposits.

sediment transport (cf. Fruergaard *et al*. 2020). Nevertheless, the formation of a spit system "resulted from complex interactions between wave and tide dynamics, fluctuations in sea level, predominantly in a sea level rising regime, the impact of storms, the high sediment supply and geological and morphological inheritance" (cf. Fruergaard *et al*. 2020, p. 502; see also Nehyba and Roetzel 2021). Spit systems are associated with retreating deltas or river mouths, estuary mouths, bedrock ridges or fault escarpments, or an abrupt change in orientation of shoreline, etc. (compare Leszczyński and Nemec 2015; Nehyba and Roetzel 2021; Spaggiari and Bordy 2023). They often grow in length in the direction of the current and can form lagoons or salt marshes behind them (cf. Hiroki and Masuda 2000; Beni *et al*. 2013; Shan *et al*. 2015).

Deposits of spit systems are interpreted as part of transgressive system tracts (Hiroki and Masuda 2000; Nehyba and Roetzel 2021). The formation of spits is favoured by a transgression, though spits may form at all stages of eustatic sea level. For the formation of spit deposits relatively stable depositional conditions are assumed, which are characterized by strong unidirectional currents, high sand supply, and sufficient accommodation space (Nehyba and Roetzel 2021).

In this study, we examine and reinterpret the quartz-kaolinitic sandstones in the Krákorka Quarry near Červený Kostelec (northeastern Bohemia, Czechia; Text-fig. 1). While the uppermost Devět Křížů Sandstone, which is highly bioturbated with trace fossils and root casts, is traditionally included in the Triassic Bohdašín Formation, it is much more similar to the overlying marine upper Cenomanian Peruc-Koryčany Formation (Tables 1 and 2). The association of biogenic structures produced by marine invertebrate tracemakers and continental plants (rhizoliths, root casts) made this locality unique in the fossil record, and has been widely cited as such (e.g., Bengtson *et al*. 2021; Knaust 2021a; Bertling *et al*. 2022). We propose and document a spit bar setting as a possible depositional environment for the uppermost Devět Křížů Sandstone based on sedimentological and ichnological records, and suggest that it was deposited in the middle/late Cenomanian rather than in the Triassic. The burrowing styles in the yellowish quartz-kaolinite sandstones, and the palaeogeographic and tectonic context, are briefly discussed. A new model of Late Cretaceous transgression that affected NW Bohemia is also proposed.

Chronostratigraphic chart			Lithostratigraphy	
System	Series	Stage	Regional substage	Formation
Triassic				Bohdašín
Permian	Lopingian	Changhsingian	Zechstein	Hiatus
				Bohuslavice
		Wuchiapingian		Hiatus
	Guadalupian	Capitanian	Upper Rotliegend II	Trutnov
		Wordian	Upper Rotliegend I	
		Roadian		
	Cisuralian	Kungurian		Hiatus
		Artinskian		Chotěvice
				Hiatus
		Sakmarian		Prosečné
		Asselian	Lower Rotliegend	Vrchlabí

Table 1. Stratigraphic chart of the Permian and Triassic of the Krkonoše Piedmont Basin in the vicinity of the Červený Kostelec area, based on Martínek and Štolfová (2009) and Zajíc (2014).

Chronostratigraphic chart				Lithostratigraphy	
System	Stage		Series	Formations	Members
Cretaceous	Santonian		CON 3 and younger	Merboltice	
	Coniacian	Middle–Upper Coniacian		Březno	
		Lower Coniacian	CON 2	Teplice	Rohatce
			CON 1		
	Turonian	Upper Turonian	TUR 7		
			TUR 6	Jizera	
			TUR 5		
		Middle Turonian	TUR 4		
			TUR 3		
		Lower Turonian	TUR 2	Bilá Hora	
			TUR 1		
	Cenomanian		CEN 6	Peruc-Koryčany	Pecinov
			CEN 3-5		Koryčany
			CEN 1-2		Peruc

Table 2. Simplified stratigraphic chart of the Upper Cretaceous showing regional lithostratigraphic units after Nadaskaý *et al*. (2019) and Nadaskaý (2021).

GEOLOGICAL SETTING

The Krákorka Quarry is located in the northern Czech Republic on a morphological elevation that subdivides the late Palaeozoic Náchod and Trutnov subbasins (Text-fig. 2). The area between Červený Kostelec and Úpice is commonly referred to as the 'U Devěti Křížů' (Wojewoda *et al*. 2016). It represents a local structural depression – the Červený Kostelec Trough – that is customarily included into the Trutnov Subbasin (Holub 1972; Uličný 2004). The lower Permian Trutnov and Bohuslavice Formations, which consist of (1) red and brown conglomerates and (2) dolomitic arkosic sandstones and mudstones with dolomite intercalations, and the Triassic Bohdašín Formation are all present in the Trutnov, Náchod and Intra-Sudetic Basins (Vejlupek 1990; Tásler 1995; Opluštil *et al*. 2016; Šimůnek 2019 and references therein; Table 1).

The studied sandstones are referred to as the Barchoviny Member, or informally as the Devět Křížů Sandstone after their type locality (Holub 1966; Uličný 2004), which belongs to the uppermost Bohdašín Formation (Prouza *et al*. 1985; Mikuláš and Prouza 1999). Mikuláš and Prouza (1999) and Čech *et al*. (2018) suggested an Early to Middle/?Late Triassic age for the studied deposits based on the discovery of a dinosaur footprint by Zajíc (1998), which is still regarded as the best chronostratigraphic constraint on the Devět Křížů Sandstone (cf. Mikuláš 2019). Zajíc (1998) reported a theropod footprint belonging to the Coelurosaria, which might suggest a younger depositional age than the Early Triassic, potentially ranging

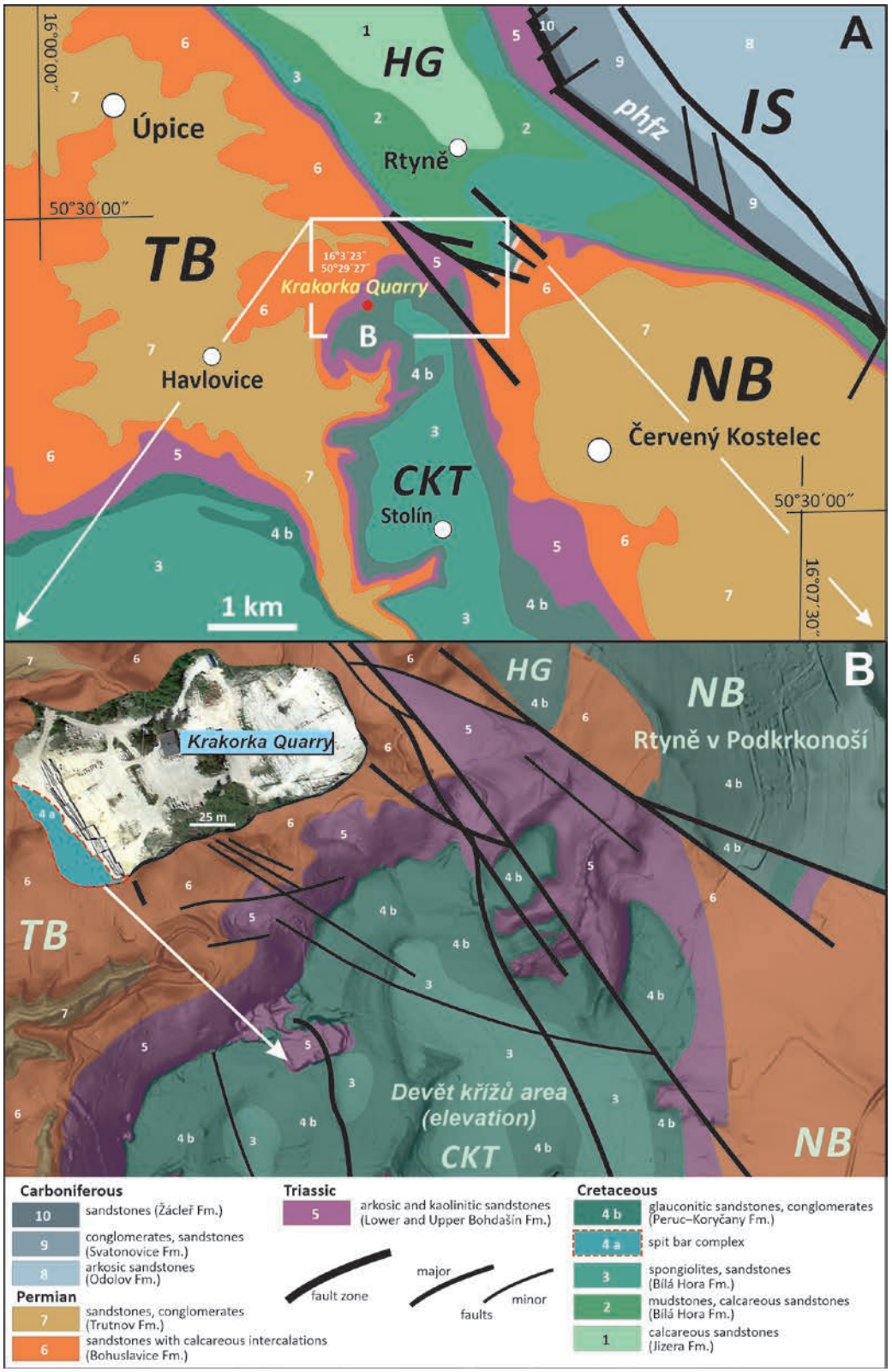

Text-fig. 2. Location of the Krákorka Quarry on the Devět Křížů morphological elevation (A), within the Červeny Kostelec structural depression (CKT) between the Trutnov (TB) and Náchod (NB) subbasins, after Opluštil *et al*. (2022 and references therein), slightly modified. Faults based on Prouza (1988). B – Cenomanian outcrop within the quarry. Explanation of symbols: HG – Hronov Graben, IS – Intra-Sudetic Basin.

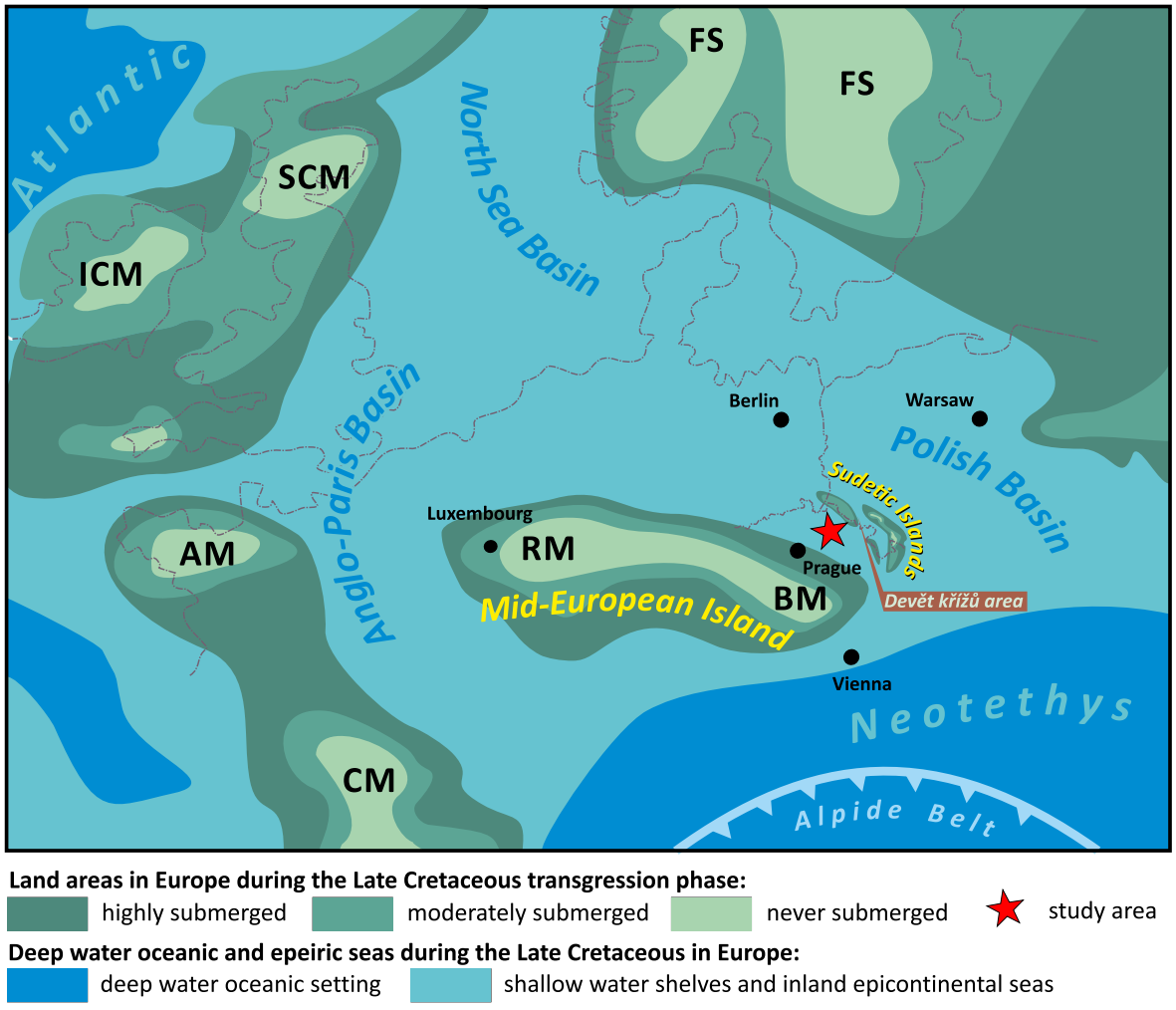

Text-fig. 3. Palaeogeography for the early Late Cretaceous (Cenomanian–Coniacian) of Central Europe, compiled after Voigt *et al*. (2008), Vejbæk *et al*. (2010) and Erbacher *et al*. (2020), modified. Explanation of symbols: RM – Rhenish Massif, BM – Bohemian Massif, CM – Massif Central, AM – Armorican Massif, ICM – Irish Caledonian Massif, SCM – Scottish Caledonian Massif, and FS – Fennosarmatian Shield.

into the Jurassic. However, Madzia (2014) suggested that this is an indeterminate dinosauromorph footprint and cannot be used as a stratigraphic marker to date the Bohdašín Formation. Indeed, a diverse assemblage of dinosauromorphs existed as early as in the Middle Triassic (Mikuláš 2019; Marchetti *et al*. 2021).

Permian, Triassic, and Cretaceous strata are exposed in close vicinity to Krákorka Quarry (Text-fig. 2; Tables 1 and 2). The basement, which lies more than 60 m beneath the quarry mining level, is composed of the youngest (uppermost lower Permian–Saxonian) continental deposits in the Central Sudetes, referred to the Bohuslavice Formation (Śliwiński 1984; Aleksandrowski *et al*. 1986; Wojewoda 2008).

The Triassic Bohdašín Formation is composed of three main lithofacies: (1) polymictic sandstones and conglomerates, (2) feldspathic sandstones, and (3) kaolinitic quartzose sandstones and conglomerates with abundant monocrystalline quartz (cf. Prouza *et al*. 1985). The first two lithofacies are intermingled, whereas the third is only present in the topmost Bohdašín Formation and is exploited in the Krákorka Quarry. The lower (1) and middle (2) Bohdašín Formation is 60 m thick, and comprises medium-grained arkosic sandstones deposited in braided river and alluvial plain environments (Mroczkowski and Mader 1985; Prouza *et al*. 1985; Prouza and Tasler 1985; Wojewoda *et al*. 2016). The upper Bohdašín Formation (3), referred to as the Devět Křížů Sandstone, is 7.5–9.5 m thick and composed of quartz-kaolinite sandstones with a distinct, regular platy parting. These deposits have been re-

garded as alluvial, lacustrine, or aeolian in origin (Valín 1964; Prouza *et al*. 1985; Mader 1990, 1992; Mikuláš *et al*. 1991; Uličný 2004), but some workers interpreted them as shallow-marine (Holub 1972; Vejlupek 1983). The Devět Křížů Sandstone is usually white-grey, passing into yellow in the uppermost portion. Additionally, these yellowish sandstones and conglomerates host abundant monocrystalline quartz and glauconite (cf. Prouza *et al*. 1985; Mikuláš and Prouza 1999; Uličný 2004). They are also heavily bioturbated. Root traces and trace fossils were recognized in these deposits by Mikuláš and Prouza (1999).

The Triassic deposits are overlain by the lower–upper Cenomanian Peruc-Koryčany Formation (cf. Nadaskaý *et al*. 2019; Nadaskaý 2021; Table 2), which consists of marine clastic deposits ("glauconitic conglomerates of the Korycany Member", cf. Mikuláš and Prouza 1999, p. 336). During the Late Cretaceous, the study area was at the periphery of the Mid-European Island, within the Saxo-Bohemian Basin (cf. Voigt 2009; Wilmsen *et al*. 2014; Voigt *et al*. 2021; Text-fig. 3).

Uličný (2004) conducted a structural and facies analysis of the sediments exposed in Krákorka Quarry, and reported an aeolian depositional environment. Additionally, Uličný (2004) described two interbedded and laterally transitional facies – dune facies and interdune facies – in the Devět Křížů Sandstone. The dune facies comprises cross-stratified sandstones, while the interdune facies consists of horizontally stratified sandstones with common mud intercalations and a variety of sedimentary and post-depositional structures, i.e., wave and ripple raindrop impressions, adhesion ripples, polygonal desiccation and syneresis cracks, and spectacular sand volcanoes (Uličný 2004; Wojewoda *et al*. 2016). Uličný (2004) interpreted the upward disappearance of interdune facies as resulting from progressive increase in sand availability, leading to the deposition of compound dunes. It is worth emphasizing that an aeolian-fluvial depositional pattern occurs throughout wide swaths of Europe in the Triassic (Mader 1982, 1983). Uličný (2004) explained the presence of trace fossils in the Devět Křížů Sandstone as resulting from Cenomanian marine bioturbation, which penetrated into the root shafts that extended through the Bohdašín and Peruc-Koryčany Formation discontinuity surface. However, he reported no plant fossils within these deposits, which is striking because vegetation should be anticipated in seasonally flooded settings.

Previously, Mikuláš and Prouza (1999) reported the occurrence of *Thalassinoides* [cf. *Thalassinoides paradoxicus* (Woodward, 1830) and cf. *Thalassinoides suevicus* (Rieth, 1932)] and *Arenicolites* isp. in the c. 2 m thick rhizolith-bearing horizon from the uppermost Krákorka Quarry. They postulated that bioturbation intensity increases towards the top of formation, which ranges to the base of the weakly lithified, oligomictic, glauconitic conglomerates of the lower Peruc-Koryčany Formation. The formation boundary surface is covered by *Thalassinoides* and root traces (Mikuláš and Prouza 1999, pl. I, fig. 2). Trace fossils assigned to *Thalassinoides paradoxicus* Kennedy, 1967 were also reported by Knaust (2021a, fig. 5F) from this erosional surface. Mikuláš and Prouza (1999) postulated that the burrows in the studied yellowish quartz-kaolinitic sandstones are Cretaceous in age. The burrowing organisms may have penetrated the yellowish sandstones up to 2 m below the discontinuity surface.

PALAEOGEOGRAPHIC BACKGROUND

In the northern Bohemian Massif, basin development and deposition occurred during the early Permian, the late Permian to Early Triassic, the Middle Jurassic to Early Cretaceous, and the Late Cretaceous (middle/late Cenomanian to early Turonian) (cf. Nádaskay *et al*. 2019). However, Valečka (2019) excluded potential deposition during the Early Cretaceous. Conversely, peneplanation and erosion took place during the Middle Triassic to Middle Jurassic and in the Early Cretaceous. During the Triassic, fluvial and lacustrine sedimentation was restricted to the western Bohemian Massif, while the Vindelic-Bohemian mainland was emergent further east (Hejl *et al*. 2023).

On the Bohemian Massif, the Late Cretaceous transgression began in the middle Cenomanian (see e.g., Wilmsen *et al*. 2014). The multi-phase sea-level rise from the middle Cenomanian to the early Turonian was responsible for the formation and preservation of thick, valley-filling strata. Recently, Wilmsen *et al*. (2019) revised the stratigraphy of the northwestern Saxonian Cretaceous Basin based on integrated palaeontological and facies analyses. The transgression was postulated to begin in the early middle Cenomanian instead of the late early Cenomanian, as assumed previously. Wilmsen *et al*. (2019) proposed that transgressive phases occurred in the early middle Cenomanian, the early late Cenomanian, and the latest Cenomanian–early Turonian, with regressive phases in the middle middle Cenomanian and middle late Cenomanian, respectively. The Saxonian and Bohemian Cretaceous Basins were first connected during the late Cenomanian, when the West Sudetic Island was separated from the mainland by a shal-

low seaway (Wilmsen *et al*. 2019; Text-fig. 3). During the Late Cretaceous, the Bohemian Cretaceous Basin formed a narrow seaway connecting the North Sea Basin and the Tethys Ocean (Voigt 2009; Čech 2011; Voigt *et al*. 2021). Several hundred metres of Upper Cretaceous marine sediments accumulated in central and northern Bohemia (Uličný *et al*. 2009). However, Špičaková *et al*. (2014) argued that due to the lack of precise bio- or chemostratigraphic criteria, individual phases of the relative sea-level record in the Bohemian Cretaceous Basin cannot be precisely correlated to other Late Cretaceous basins. Recently, Nadaskaý (2021) postulated that the main transgressive pulse at the Cenomanian–Turonian boundary is recorded in both Saxonian and Bohemian basins.

The Late Cretaceous transgression resulted in various diachronous deposits, ranging from the middle/late Cenomanian to the early Turonian, across the Sudetes. Depending on the timing of flooding, and the local topographic and geological characteristics (for instance, weathering, local palaeoslope inclination), different sedimentary styles resulted. For example, in the Cenomanian, areas with the older sedimentary substrate (Intra-Sudetic Synclinorium, Náchod and Trutnov Basins), were generally characterized by fining-upwards deposition.

Elsewhere, in localities that were submerged only in the early Turonian (e.g., Orlicka Island, Nove Mesto), the Cretaceous succession begins with a 10–15 cm thick gravel cover on the crystalline substrate, passing into fine-grained calcareous and siliceous deposits. Only after the maximum Cretaceous transgression in the early Turonian, and subsequent regressive-progradational episodes, did the palaeotopographic conditions become uniform across the entire basin, as documented by Cretaceous deposits in the Saxonian facies on the northern and northwestern peripheries of the Bohemian Massif.

According to Valečka (2019), the remnant Jurassic deposits on the West Sudetic Island supplied debris to the Bohemian Cretaceous Basin, and diagnostically Jurassic clasts are found in Upper Cretaceous to Neogene deposits, for instance, in the Coniacian sandstones of north Bohemia. In the Jurassic, fluvial, deltaic, and nearshore clastic sedimentation in the Bohemian Massif began on its southeastern slopes in the Bajocian to Bathonian, and extended to north Bohemia and Saxony in the latest Callovian (Valečka 2019). Subsequently, the early Kimmeridgian and Oxfordian transgressive phase from the northern Tethys led to the development of a Jurassic seaway across much of the Bohemian Massif, and the connection of its southeastern margin with north Bohemia and Saxony (cf. Valečka 2019).

METHODS

Sedimentary structures, burrows, and root traces were described, measured and photographed in the field. Laboratory descriptions of collected trace fossil specimens were supplemented by detailed photographs. Bioturbation indices (BI) or the bedding-plane horizontal index (BPHI after Dorador and Rodríguez-Tovar 2014), which reflect the extent of bioturbation on originally horizontal bedding-planes, were quantified *in situ* on exposed horizontal surfaces in 0.5×0.5 m grids, following Miller and Smail (1997). This scheme resembles closely the method of Droser and Bottjer (1986) for evaluating ichnofabric as represented on vertical surfaces and facilitate comparison between horizontal and vertical exposures (cf. Dorador and Rodríguez-Tovar 2014; Tables 3 and 4).

Horizontal bedding-plane bioturbation indices range from BI = 0 (without bioturbation) to 5 (homogenized sediment with no primary sedimentary

Bedding-plane bioturbation indices (BI)	Disruption of bedding planes by the activity of organisms (%)	Bioturbation	Description
1	0		No bioturbation.
2	0–10	sparse bioturbation	Bioturbation may be represented by zones of generalized disruption or by discrete trace fossils. Most discrete structures are isolated, but some intersect.
3	10–40	low bioturbation	Bioturbation represented by discrete traces, zones of generalized disruption, or by both.
4	40–60	moderate bioturbation	Bioturbation represented by discrete traces, zones of generalized disruption, or by both. Interpenetration of discrete structures is more common than in less bioturbated surfaces.
5	60–100	high bioturbation	This includes bedding planes in which up to 100% of the bedding plane Surface has been disrupted by the activity of animals.

Table 3. Diagram of bedding-plane bioturbation indices according to Miller and Smail (1997).

Ichnofabric indices (ii)	Disruption of ichnofabric by the activity of organisms	Bioturbation	Description
1	0%		No bioturbation recorded; all original sedimentary structures preserved.
2	up to 10%	sparse bioturbation	Discrete, isolated trace fossils, up to 10% of original bedding disturbed.
3	10–40%	low bioturbation	Approximately 10 to 40% of original bedding disturbed. Burrows generally isolated, locally overlapping.
4	40–60%	moderate bioturbation	Last vestiges of bedding discernible; approximately 40 to 60% disturbed. Burrows overlap and are not always well defined.
5	60–up to 100%	high bioturbation	Bedding completely disturbed, but burrows are still discrete in places and the fabric is not mixed.

Table 4. Diagram of ichnofabric indices after Droser and Bottjer (1986).

structures, interpreted as complete bioturbation; see Table 3). While the bioturbation index is commonly measured in marine sequences, it has been adapted for continental deposits, for instance paleosols with insect burrows (Genise *et al*. 2004; Hsieh and Uchman 2023; Nascimento *et al*. 2023). Ichnofabric indices (ii after Droser and Bottjer 1986; see also Taylor and Goldring 1993; Taylor *et al*. 2003), based on the percentage of ichnofabric disturbance by trace fossils, were measured on vertical surfaces in 0.5×0.5 m grids. In this scheme, ii = 1 means no bioturbation (0%), whereas ii = 5 means completely disturbed bedding with still occasionally discrete burrows (60–100%). In this scheme, burrows can locally overlap at ii = 3, and cross-cutting (burrow overlap) is common at ii = 4 (see Table 4).

Rhizoliths mainly occur as root casts. Their characteristics, i.e., length, thickness, branching angle and colour, were described following Klappa (1980), Retallack (1988), and Kraus and Hasiotis (2006).

LITHOLOGY OF THE UPPERMOST DEVĚT KŘÍŽŮ SANDSTONE

The sandstones and conglomerates of the uppermost Devět Křížů Sandstone reach a total thickness of up to 2.2 m (Text-fig. 4). In Krákorka Quarry, it is possible to distinguish 3 distinct, compound units forming a characteristic sequence: (1) a lower (basal) conglomerate, (2) a lower compound conglomeratic sandstone layer, and (3) an upper compound sandstone-to-conglomerate layer.

Section 1 – Lower (basal) conglomerate – residual lag (6–7 cm)

The sequence begins with a quartz gravel conglomerate, with a maximum clast size of <2 cm and a kaolinitic cement (Text-fig. 5A). The grains are matrix supported, very well rounded and not oriented. The normal grading of the gravel fraction is weakly marked, and the transition to the overlying sediments is gradual. Rhizocretions continue throughout the conglomerate layer, and probably extend up to the top of the Lower Triassic deposits.

Section 2 – Lower compound conglomeratic sandstone layer (1.35 m)

Directly above occurs a compound conglomeratic sandstone layer, with a composition varying from quartz arenite to lithic subarkose with clay cements composed mostly of illit (Text-figs 4, 5B). The pebbles are less than 1.5 cm in diameter. In the lower part, this layer shows only relics of primary bedding, with abundant plant (rhizoliths) and invertebrate (trace fossils) bioturbation. There are abundant clayey intraclasts with vermiculite locally showing clear (pseudo?) imbrication fitting to the bedding relics (Text-fig. 5E). Above, the sediment is clearly stratified, with the dominant inclination of low-angle bedding surfaces (<15º) ranging between ~300º and 20º (Text-fig. 5C). There are numerous clay intraclasts that show clear current imbrication on slightly inclined reactivation surfaces, suggesting northwards intraclast transport (Text-figs 5E, 6C, D). In some places, clay material is so abundant that the sediment gives the impression of a uniform, lenticular clay level – only bedding surface observations reveal the presence of numerous intraclasts. The upper part of the layer is clearly cross-bedded. In sets, up to 0.5 m thick, cross tangential bedding dominates and dips at approximately 270º to 320º (Text-fig. 5B–D). Differently oriented erosional surfaces are common in this part of the profile, over which sedimentation evidently reactivates. Listric shaped surfaces incline in the same direction as the co-set cross-bedding, as well as low-amplitude trough surfaces with transverse axes of predominate layering. Reactivation

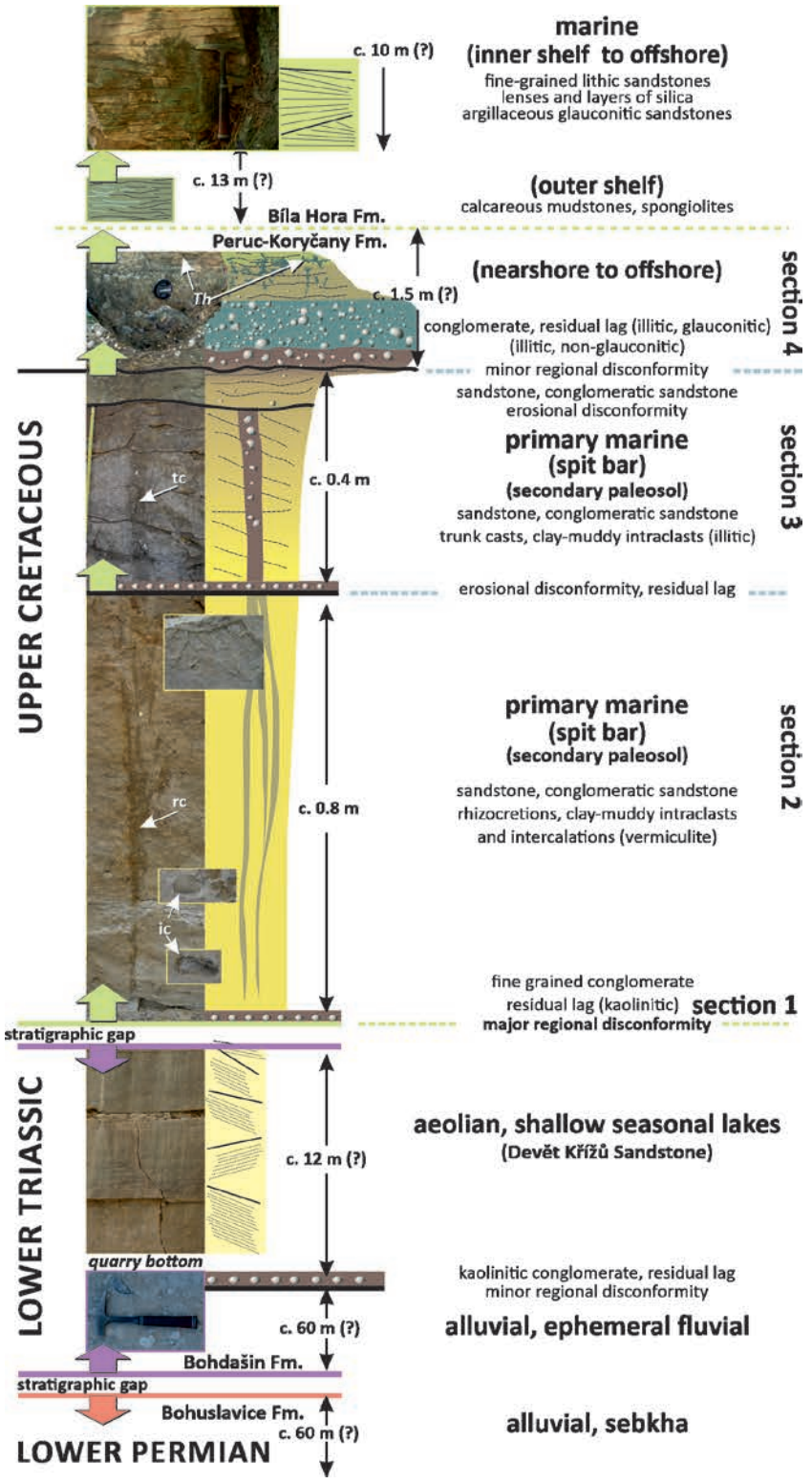

Text-fig. 4. Generalized lithostratigraphic profile in the Krákorka Quarry, with lithologic characteristics, approximate thickness, and generalized sedimentological and/or environmental interpretations. Lithostratigraphy of the Cretaceous is applicable only to the near vicinity of the quarry. Numbers 1–4 refer to individual sections, for details see text; Bohdašin Formation: section 1 – lower basic conglomerate – residual lag; section 2 – lower compound conglomeratic sandstone layer; section 3 – upper compound sandstone-and-conglomerate layer; section 4 – marine transgressional sequence of the Peruc-Koryčany Formation. Abbreviations: tc – trunk casts, rc – root casts; ic – clay intraclasts, *Th* – *Thalassinoides*.

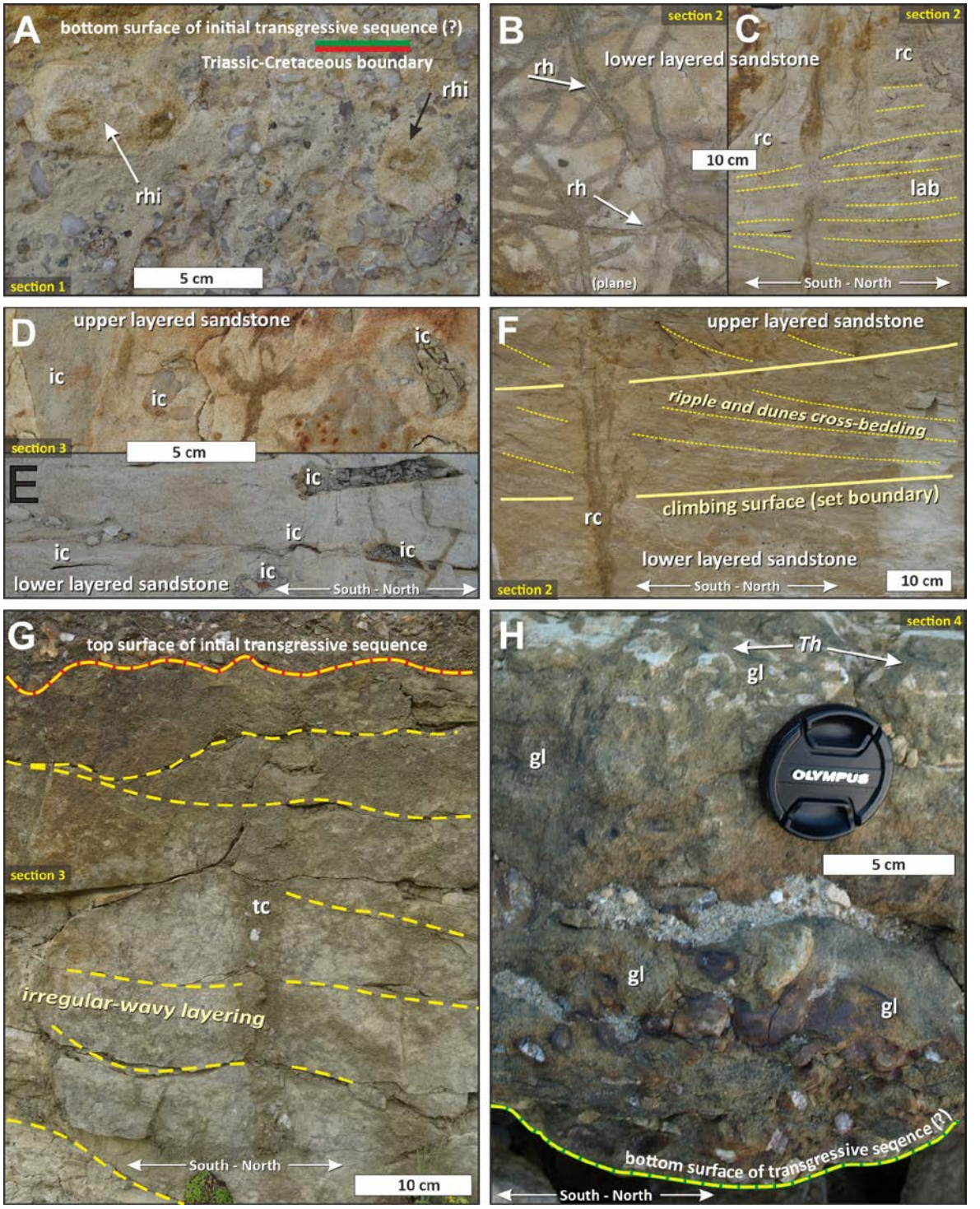

Text-fig. 5. Main features of the spit facies complex sediments. Explanations: lab – low angle sandstone member; gl – glauconite; rhi – rhizocretions; rh – rhizoliths; for remaining abbreviations see Text-fig. 4. A – Rhizocretions cutting the lowermost conglomeratic member (1) of the spit bar complex. B – Rhizoliths on sandstone bedding surface, lower layered sandstone (2). C – Yellow conglomeratic and cross-bedded sandstones (2), low angle sandstone member. D – Rounded clay intraclasts in the upper layered sandstones (3). E – Angular clay intraclasts on the erosional reactivation surfaces of the bottom spit bar complex, upper layered sandstones (3). F – Ripple and dune cross-bedded sandstone of the inner spit bar complex, lower upper layered sandstones (2, 3). G – The uppermost non-glauconitic conglomeratic member with buried trunk casts and buried irregular beddings (3). H – Basal transgressional conglomerate and intensely bioturbated glauconitic conglomeratic sandstone, representing a local transgressional facies (4). C, E–H – cross-sections; A, B, D – planar views. Explanations of individual sections 1–4 as in Text-fig. 4.

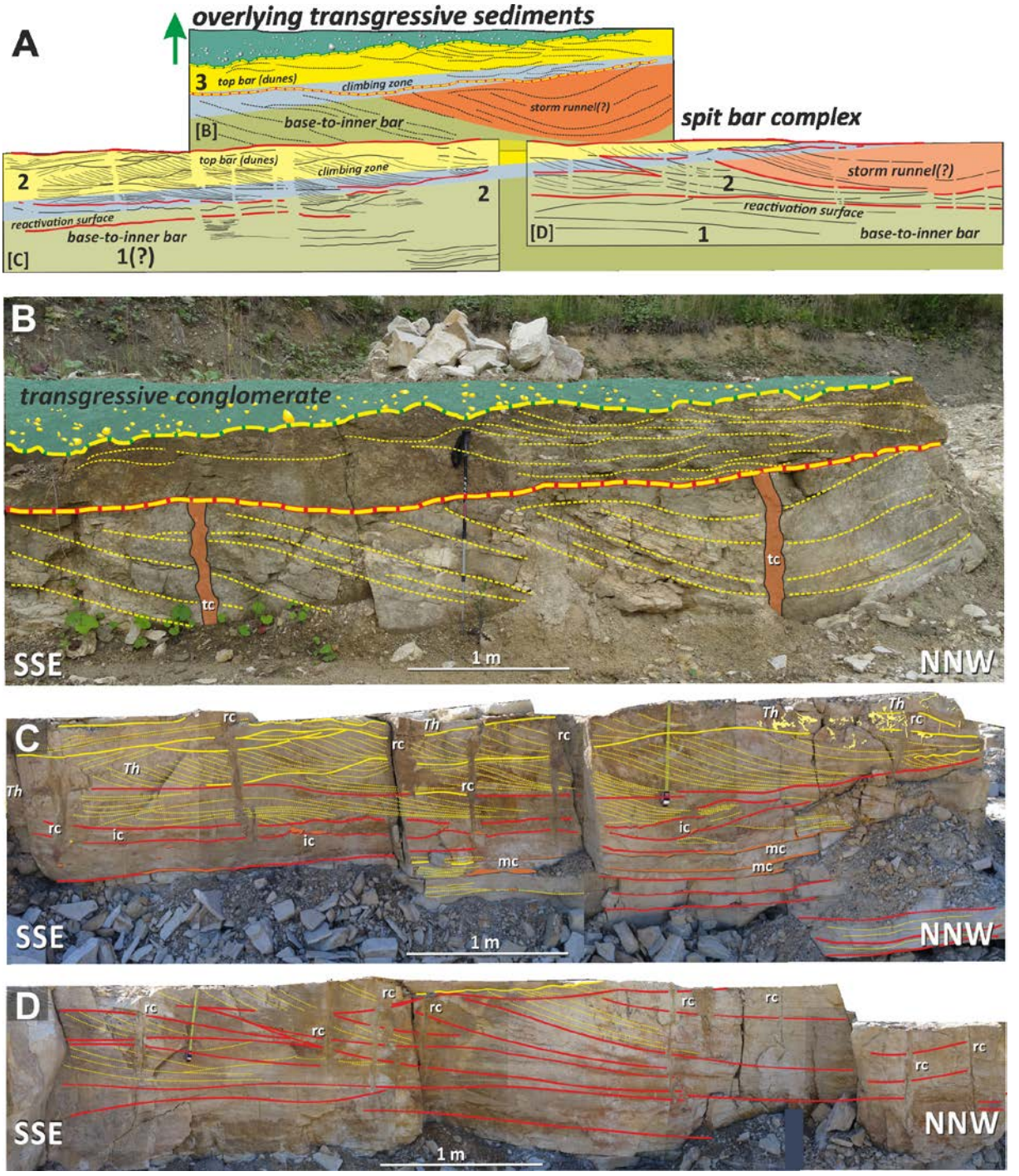

Text-fig. 6. Three main *in situ* sections interpreted here as a spit bar facies association. Expanations: mc – muddy cover; other abbrevations as in Text-figs 4 and 5. A – Site geometry (B, C, and D) and their most probable spatial arrangement. B – Uppermost Devět Křížů Sandstone Sandstone with trunk casts. C, D – Upper part of the Devět Křížů Sandstone with root casts. Lines indicate stratification: yellow dashed – ripple and dune cross-bedding on various scales; solid yellow – non-erosional climbing surfaces and boundaries of diagonal layered sets; red – erosional reactivation surfaces, locally covered by mud carpets; red-yellow dashed – lower border of the 'basic transgressional conglomerates' and green-yellow dashed – lower boundary of glauconite and/or chamosite bearing sediments.

surfaces are often covered with continuous clay covers (not intraclast accumulation), up to 3 cm thick (Text-fig. 6C, D). The whole layer is intersected by root casts accompanied by invertebrate bioturbations

(Text-figs 5C, F, 6C, D). The lower compound conglomeratic sandstone layer is topped by an erosional surface and covered with a thin, less than 5 cm thick polymictic conglomerate.

Section 3 – Upper compound sandstone-and-conglomerate layer (65 cm)

Above occurs another compound layer, composed mostly of coarse-grained to conglomeratic lithic arenite, with illite and/or silica cement (Text-fig. 4). The maximum clast size is up to 2 cm. This layer shows inverse grading in both the sandy and gravely fractions. Primary bedding relics are very poorly preserved; in the Krákorka Quarry, they create irregular, wavy surfaces that are dominantly inclined towards the north (Text-fig. 5G). Within the layer, there are vertically-oriented cylindrical structures, most likely traces of buried woody plant trunks, filled with coarser-grained, mostly gravelly clasts. The layer is topped with a polymictic conglomerate member, and the boundary between the conglomeratic sandstone and the capping conglomerate is not erosive. Thus, it is difficult to unambiguously determine if this constitutes a separate unit of distinct origin. The material in the conglomerate is the same as that filling the trunk-related voids, but due to the lack of a basal erosive surface it does not represent a typical residual lag. Instead, it rather resembles proximal tempestite deposits that formed at the base of nearshore bars (see Einsele *et al*. 1991; Myrow and Southard 1996; Tiffany *et al*. 2013). It may be associated with conglomerates of the overlying marine Peruc-Koryčany Formation, but does not contain glauconite and was probably deposited under different conditions. Therefore, they may be a record of the initial, high-energy stage of transgressive sediment developments as the erosional base (i.e., wave base) gradually rose.

Section 4 – Marine transgressional sequence of the Peruc-Koryčany Formation

The Krákorka Quarry profile is capped by a similar polymictic conglomerate, up to over 5 cm thick, to that ending the initial transgressive sequence, except that it contains abundant glauconite and chamosite (cf. Text-figs 4, 5H). Moreover, the boundary between the previous conglomerate and this conglomerate is very distinct and presumably erosive. This conglomerate has been commonly referred to as the "glauconitic conglomerate" of the upper Cenomanian Peruc-Koryčany Formation (cf. Mikuláš and Prouza 1999, p. 336). In Krákorka Quarry, the conglomerate reaches a maximum thickness of approximately 25 cm, transitioning upwards into a very strongly bioturbated, medium-grained lithic greywacke. About 25 m from the quarry, conglomerates of the upper Cenomanian Peruc-Koryčany Formation pass up into mudstones, fine-grained sandstones, spongiolites, and finally argillaceous glauconitic sandstones (Lower Quadersandstein megafacies) of the lower Turonian Bílá Hora Formation (Text-figs 2, 3; Table 2).

Sediment architecture

The lower structural assemblage ('base to inner bar'; 'number 1' in Text-fig. 6A, C, D) consists of coarse-grained sandstone co-sets, with cross-stratification resembling apparent hummocky cross-stratification (HCS), cut with low-angle erosional surfaces, and covered with clay or mud. The central assemblage ('number 2' in Text-fig. 6A, C, D) consists of multiple planar or trough cross-bedded sets that represent current ripple and dune deposits (Text-fig. 5F). The sets are arranged in a climbing system and the set boundaries incline opposite to the bedding direction, which generally shows a northwards palaeotransport – i.e., nearly opposite to the regional palaeoslope inclination (Text-fig. 5F). In places, at the base of the sets, there are numerous accumulations of sharp-edged clay-and-mud intraclasts that are characteristically parallel to the bedding planes (pseudoimbrication) (Text-figs 5D, 6C). All of these structures are cut by reactivation surfaces, which commonly feature irregular (rimmed) intraclasts showing locally characteristic current imbrication (Text-fig. 6A). Some reactivation surfaces are covered with a <3 cm thick continuous clay-mud layer (Text-fig. 6C). Moreover, the greatest concentrations of biogenic structures occur in the vicinity of reactivation surfaces. The topmost bar deposits ('number 3' in Text-fig. 6A), predominantly developed as structureless sandstones and conglomerates, are preserved only in the highest third of the succession. They most probably represent residual pavements that initiate the overlying transgressional sequence. However, they also include well-preserved buried trunk traces (Text-figs 5G, 6B), which continue downwards as rhizocretions to the top of the older, kaolinitic Triassic sandstones.

DESCRIPTION OF PLANT TRACES

In the studied deposits, rhizoliths are the main organic structures and usually occur as root casts with or without branching (Text-figs 7–11). Buried trunk

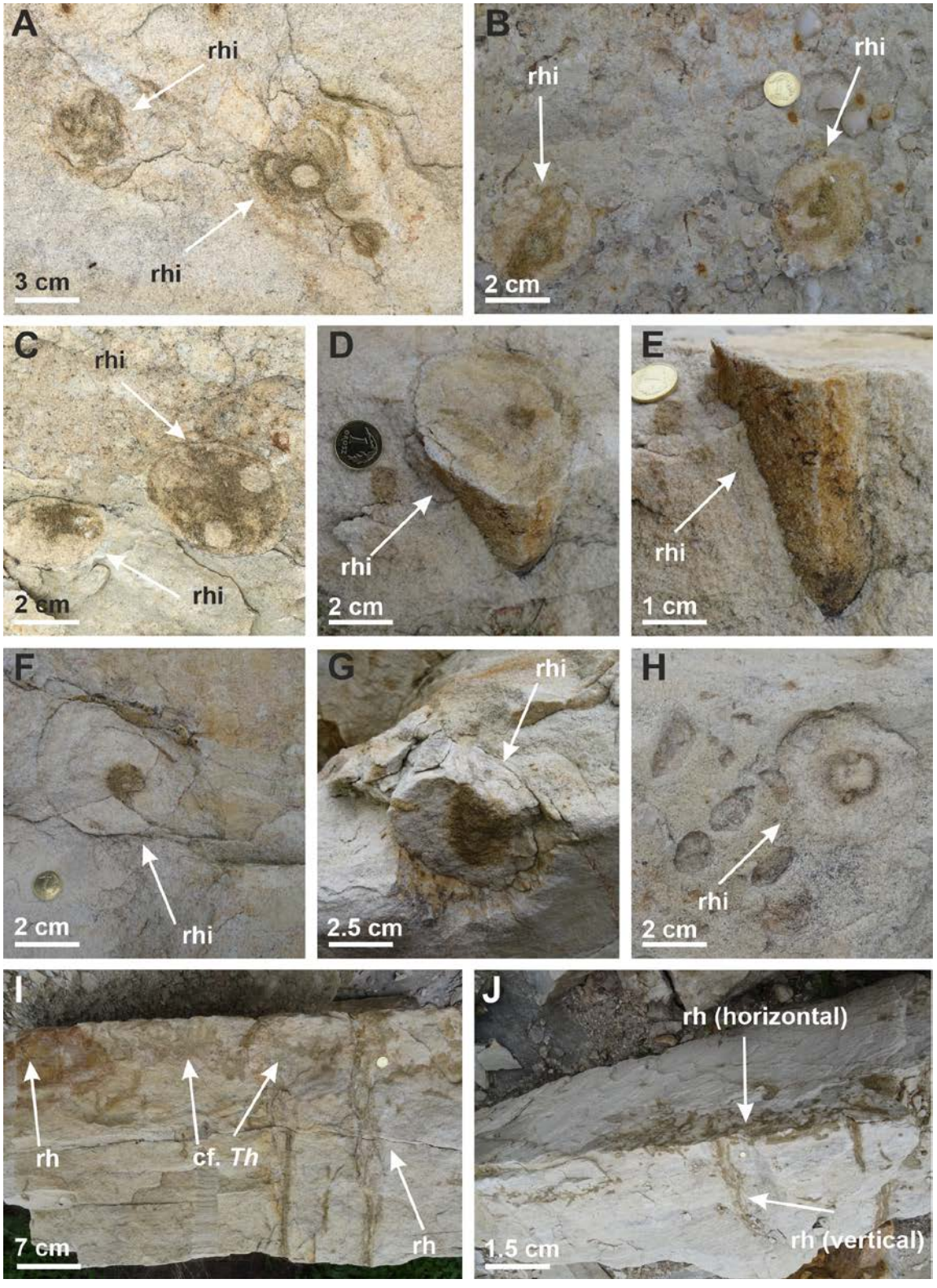

Text-fig. 7. Rhizocretions and root traces from the Krákorka Quarry. Abbreviations: rhi – rhizocretions, rh – rhizoliths, cf. *Th* – cf. *Thalassinoides* isp. A–C – Root cross-sections (rhizocretions) preserved on conglomeratic sandstone surfaces. D–H – Cross-sections of root traces (rhizocretions) preserved on sandstone bedding planes, D and E show the same specimen. I – Vertical roots (rhizoliths) in a sandstone block and cf. *Thalassinoides* isp. J – Horizontal and vertical rhizoliths preserved on sandstone bedding plane.

casts also appear, as well as horizontal networks of bifurcated root traces and unrecognizable ovoid structures. Following Klappa (1980), and Kraus and Hasiotis (2006 and references therein), rhizoliths are defined as organo-sedimentary structures that preserved plant root activity (see also Sarjeant 1975). While they were previously recognized as trace fossils, root traces are not presently considered as such (see Bertling *et al*. 2006, 2022).

Vertical root casts
(Text-figs 7, I, J, 8A–K, 10D, F–H, 11A–H)

MATERIAL: 30–40 specimens, including 3 fossil trunks.

DESCRIPTION: Simple cylindrical to subcylindrical, downward tapering structures, which are mostly vertically oriented, up to 1.5–1.6 m in length and usually 1–2 cm in width (Text-fig. 8D–G). The majority are unbranched, but some possess finer horizontal branches. These off-branches that radiate from the central axis also show a decreasing diameter. The main roots are predominantly vertical, while the offshoots are mostly horizontal. They are filled with a grey-greenish, fine-grained sand. Some fossil trunks, 90 cm long and 8–9 cm wide, also appear in the top portion of these sandstones (Text-fig. 8A–C).

REMARKS: The studied simple, cylindrical, predominantly vertically oriented structures that taper downward are identified as root casts (cf. Klappa 1980). Similar structures were reported by Mikuláš and Prouza (1999, pl. I, fig. 1, pl. IV, fig. 1) from the studied deposits and described as ?root canals. Earlier, Mader (1990) interpreted the root traces from the Krákorka Quarry as conical lycopod plant stems.

Rhizocretions
(Text-fig. 7A–H)

MATERIAL: 10–20 specimens mainly observed in the first conglomerate bed (Text-figs 5A, 7A–H). They are vertically oriented in relation to the bedding-plane.

DESCRIPTION: Circular to elliptical cross-sections visible on the bedding plane. Concentric (Text-fig. 7A, B), conical, downward tapering structures (Text-fig. 7D, E). Their upper surfaces are usually flat and slightly concave with rounded edges (Text-fig. 7D, F). In the middle of each specimen, there is a root canal up to 1 cm in width (Text-fig. 7D, F–H). However, in the specimen figured in Text-fig. 7C, two circular root canals are visible. Their diameter ranges from 3 to 6 cm, usually 4 cm, while the visible length ranges up to 5 cm. These structures are beige or rusty brownish.

REMARKS: The presence of circular to elliptical transverse outlines, and in lateral view conical-shaped concentric structures with preserved centric or eccentric axial tunnels suggests an assignment to rhizocretions (cf. Knaust 2015; Bojanowski *et al*. 2016; Uchman *et al*. 2023, fig. 15). These structures are interpreted as having formed around plant roots (cf. Klappa 1980, 2006) due to the precipitation of calcium carbonate, iron oxyhydroxides, and/or other iron minerals in the soil (cf. Uchman *et al*. 2023). According to Uchman *et al*. (2023), ferruginous concentrations around the central tunnel are typical of pedogenic processes (Text-fig. 7A). Previously, Mikuláš and Prouza (1999, pl. IV, figs 2–5) interpreted such structures as "complexly filled or thick-lined ?root canals." In Chrząstek and Wojewoda (2022) and Wojewoda *et al*. (2022), some root traces (here identified as rhizocretions) from Krákorka Quarry were incorrectly assigned to the Rosselichnidae. Similar rhizocretions were reported by Nascimento *et al*. (2023, pl. 5B) and Uchman *et al*. (2023, figs 6A–E, 7, 12C) from ancient and modern paleosol settings, including loesses and other fine-grained deposits. Uchman *et al*. (2023) described enigmatic structures ('rhizoclasts') from shallow-marine Miocene deposits of Hungary, which were interpreted as rhizocretions redeposited from another terrestrial environment. Nascimento *et al*. (2023) reported rhizocretion levels with stacking patterns that occur between different depositional crevasse splay deposits within a paleosol. The ferruginuous rhizocretions usually developed on living roots in a moderate climate with both oceanic and continental influences, under fluctuating water table and oxygen conditions (cf. Uchman *et al*. 2023 and references therein).

Horizontal rhizoliths
(Text-figs 7J, 8L, M, 9B, C, E, F)

MATERIAL: Observed usually on sandstone bedding-planes, where they occur in abundance.

DESCRIPTION: The specimens show numerous Y-shaped branching patterns. In some cases, a terminal tapering of rhizoliths was observed (Text-fig. 9E, F). The rhizolith diameters range from 0.5–1 cm to 2–8 cm, and lengths from 50–70 cm to 150–160 cm.

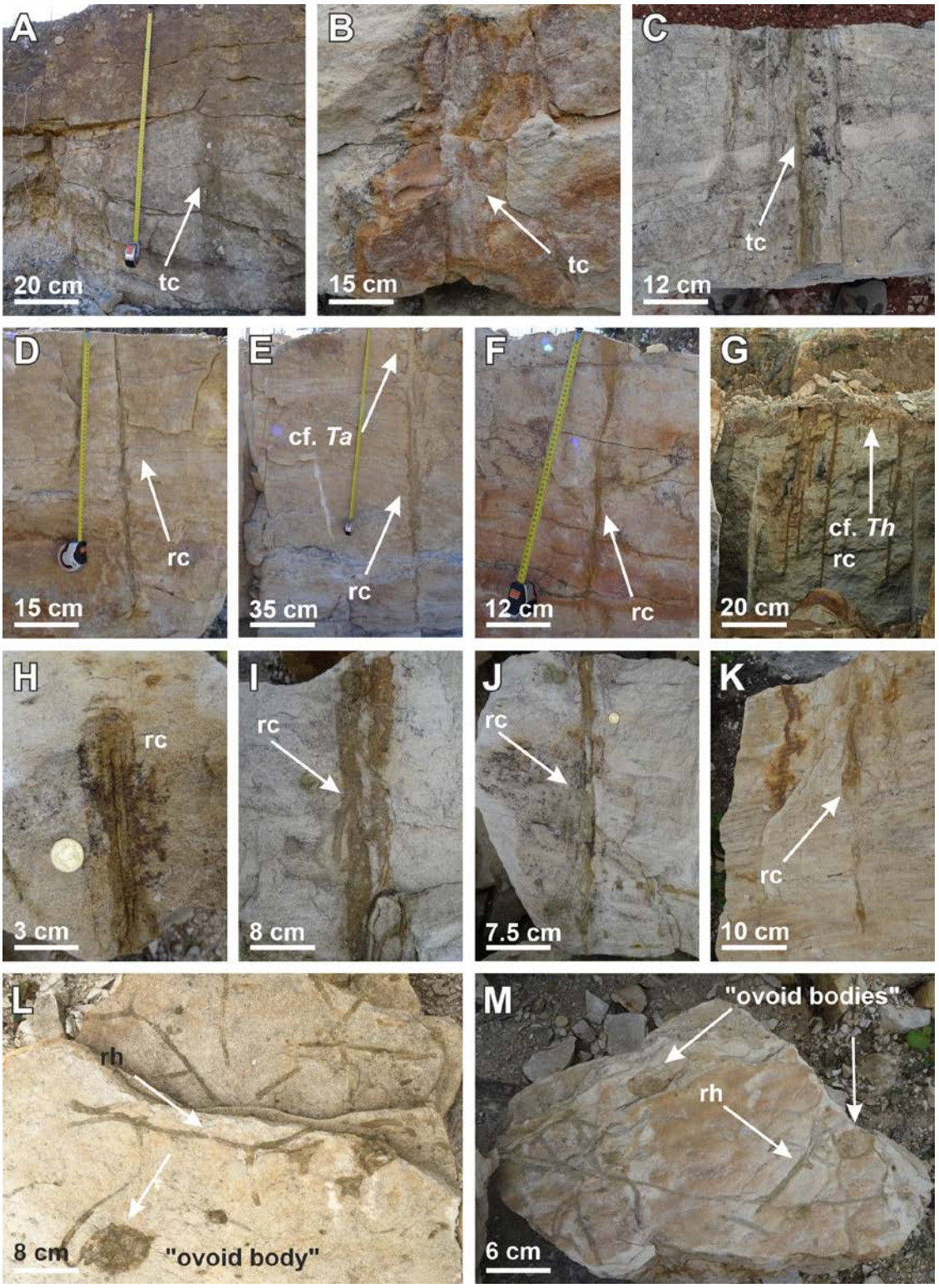

Text-fig. 8. Vertical and horizontal rhizoliths from the uppermost Devět Křížů Sandstone. Explanations: tc – trunk casts, rc – root casts, cf. *Ta* – cf. *Taenidium* isp.; other abbreviations as in Text-fig. 7. A–C – Vertical buried trunk casts up to 90 cm in length and up to 10 cm in width, visible on the sandstone wall. Some gravel inside the tree trunk. D – Vertical root cast resembling *Skolithos*. E–G – Vertical roots with burrows: cf. *Taenidium* isp. and cf. *Thalassinoides* isp. H – Vertical rhizolith similar to *Cylindrichnus*. I–K – Vertical rhizoliths with small horizontal branches. L, M – Horizontal rhizoliths and 'ovoid bodies'.

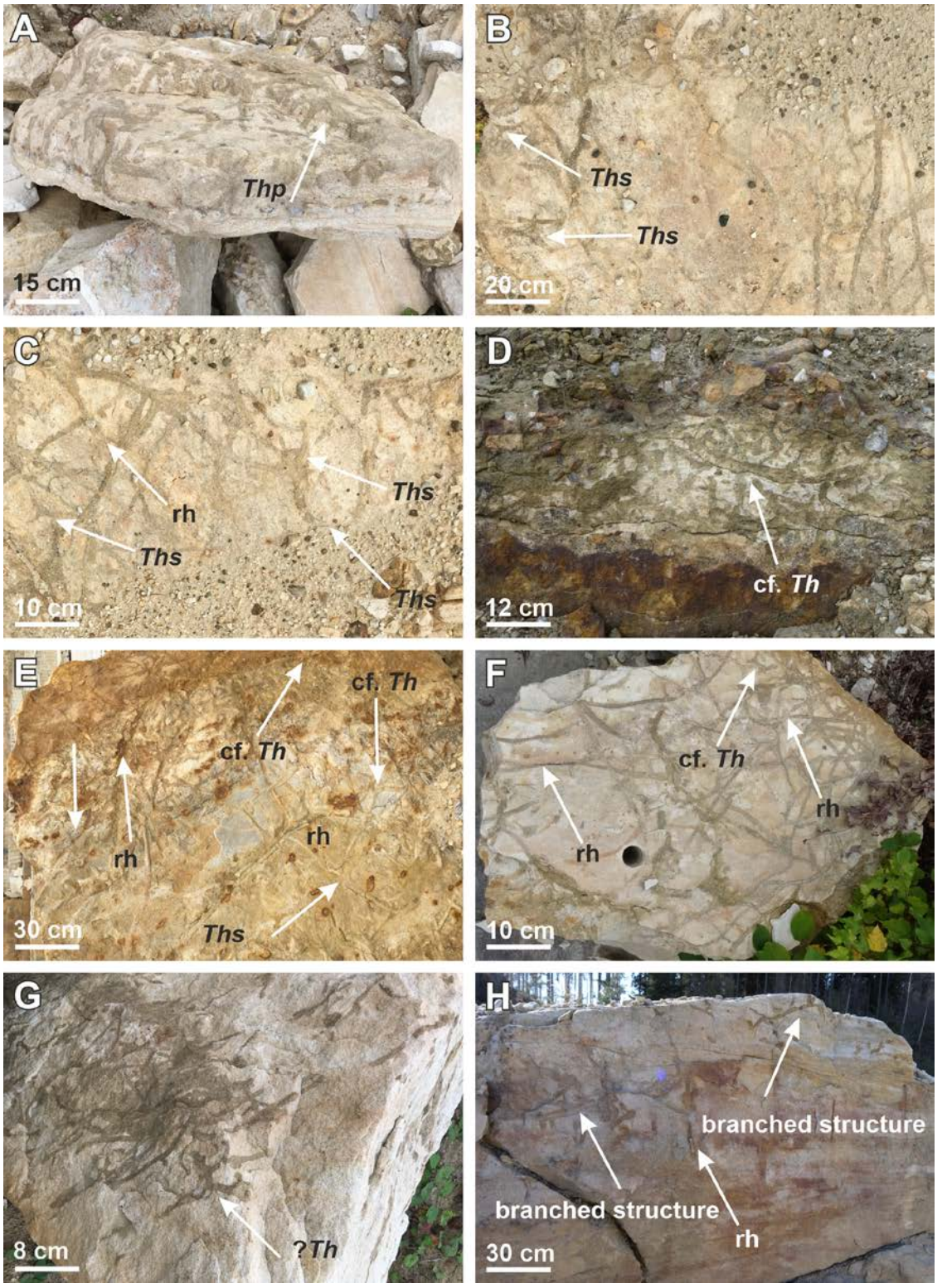

Text-fig. 9. *Thalassinoides paradoxicus* and *T. suevicus* associated with horizontal rhizoliths. Explanations: *Thp* – *Thalassinoides paradoxicus*, *Ths* – *Thalassinoides suevicus*, ?*Th* – ?*Thalassinoides* isp.; other abbreviations as in Text-figs 7 and 8. A – *Thalassinoides paradoxicus* at the boundary between the Bohdašín and Peruc-Koryčany Formations. B, C – *Thalassinoides suevicus* preserved on a bedding plane. D – *Thalassinoides suevicus* and cf. *Thalassinoides* isp. E, F – Horizontal rhizoliths and cf. *Thalassinoides* isp. on a sandstone slab surface. G – ?Horizontal network of ?*Thalassinoides* isp. tunnels. H – Branched structures and rhizoliths visible on sandstone wall.

REMARKS: Sedorko *et al*. (2020, fig. 5G) and Knaust (2017, fig. 5.182a) reported similar horizontal rhizolith network systems, with bifurcations at bedding planes. Mikuláš and Prouza (1999, pl. III, figs 1, 2) reported horizontal ?root canals from the studied deposits.

Unrecognized ovoid structures
(Text-fig. 8L, M)

MATERIAL: 4 specimens; cross-sections of ovoid unrecognizable structures on bedding planes in close association with horizontal rhizoliths.

DESCRIPTION: These structures, in some cases elliptical, are up to 8 cm diameter. It seems that they contain rhizoliths (Text-fig. 8L).

REMARKS: Knaust (2015, fig. 7E) reported similar caliche nodule structures that contain rhizolith root traces from Triassic fluvial deposits in Bornholm, Denmark. D'Alessandro *et al*. (1993) also reported ovoid bodies and interpreted them as possible plant components, parasites, or termite nests. According to Genise *et al*. (2010) and Genise (2016, 2019), ovoid structures referred to as 'rhizolith balls' are subspherical carbonate balls composed of a dense rhizolith mass, and possibly represent evidence of insect agriculture, the first described from Lower Cretaceous deposits. Chakraborty *et al*. (2013) postulated that their common association with carbonate nodules may be indicative of rhizoliths.

SYSTEMATIC ICHNOLOGY

A low diversity trace fossil assemblage was recognized, comprising *Thalassinoides paradoxicus*, *T. suevicus, Thalassinoides* isp., cf. *Thalassinoides* isp. and cf. *Taenidium*. Some indeterminate trace fossils resembling *Arenicolites* and *Beaconites* were also observed. However, due to their poor state of preservation, they are left in open nomenclature at the present time. The ?*Taenidium* ichnofabric was reported for the first time from these deposits.

Taenidium Heer, 1877
cf. *Taenidium* isp.
(Text-figs 8E, 10A–D, F–I, 11E, G)

MATERIAL: Several specimens in close vicinity to root traces, but also at some distance from rhizoliths.

DESCRIPTION: Unwalled, unbranched cylindrical straight to curved burrows with poorly defined menisci. Cross-sections of these backfilled structures are circular. Burrow courses mostly vertical and inclined, especially in association with rhizoliths, less commonly horizontal. True branching was not observed, but rare secondary branching and/or false branching caused by cross-cutting relationships of individual specimens were observed (Text-fig. 10A, G). In some cases, especially in close association with roots, burrows form dense networks. The diameter of the studied specimens is usually about 1 cm, while length varies from a few to several centimeters. The burrows are rusty-dark brown.

REMARKS: The burrow morphology is consistent with ichnotaxobases of *Taenidium*, especially *T. barretti* Bradshaw, 1981 (cf. Keighley and Pickerill 1994). They are similar to the *T. barretti* burrows described by Nascimento *et al*. (2023, figs 3G, H, 6G). However, in the majority of specimens that resemble *Taenidium*, the menisci are poorly visible and/or the presence of menisci is doubtful. False branchings due to overlapping trace fossils, which are characteristic of *Taenidium* specimens, are also common (compare Nascimento *et al*. 2023). Due to the poor state of preservation and subtly marked menisci, the studied burrows are left in open nomenclature as cf. *Taenidium*.

This meniscate backfilled burrow is regarded as fodinichnion or pascichnion (D'Alessandro and Bromley 1987; Fürsich *et al*. 2018). A combination of different behaviours, such as detritus-feeding, locomotion and dwelling, is proposed for the *Taenidium* tracemakers (cf. Rodríguez-Tovar *et al*. 2016). It characterizes the marine *Cruziana* ichnofacies (MacEachern *et al*. 2007, 2012) and the freshwater *Scoyenia* ichnofacies (Nascimento *et al*. 2023). Trace markers are postulated to be oligochaetes, myllipeds, myriapods, crustaceans, cicada nymphs, earthworms and beetle larvae (Verde *et al*. 2007; Nascimento *et al*. 2023 and references therein). *Taenidium* is a widespread ichnogenus in both marine and terrestrial deposits (Bengtson *et al*. 2021). An association between *Taenidium* and root casts was recognized previously by D'Alessandro *et al*. (1993), who described the close association of *Taenidium* and vertical roots, in which burrows were clustered tightly around the plant traces, in some cases up to more than 1 m below the sediment-water interface. In continental settings, *Taenidium* is known from crevasse splay deposits, floodplain deposits, lakes, fluvial channels and eolian deposits (Keighley and Pickerill 1994; Knaust 2015; Sedorko *et al*. 2020; Nascimento *et al*. 2023). It ranges from the Cambrian to the Recent (Mángano and Buatois 2016).

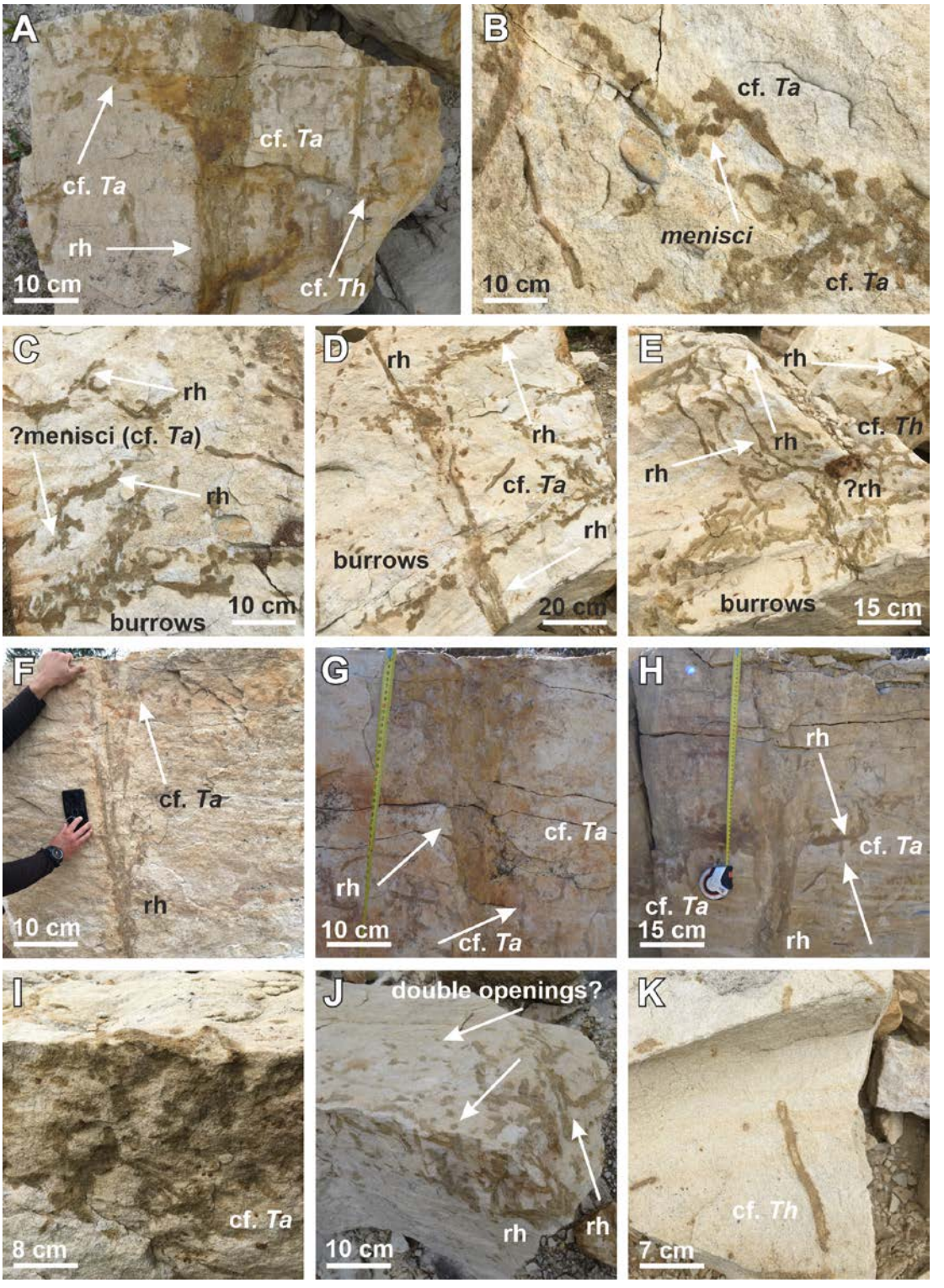

Text-fig. 10. *Taenidium* suite and root casts. Explanations: ?rh – ?rhizoliths; other abbreviations as in Text-figs 7 and 8. A – cf. *Taenidium* isp. tunnels, cf. *Thalassinoides* isp. and rhizoliths. B, C – Poorly visible menisci in cf. *Taenidium* ichnofabric. Trace fossils arranged along vertical rhizoliths. D – Vertical and horizontal fragmentarily preserved rhizoliths, and burrows resembling cf. *Taenidium* isp. E – Rhizoliths and burrows similar to cf. *Taenidium* isp. and cf. *Thalassinoides* isp. F–I – cf. *Taenidium* ichnofabric in close vicinity to rhizoliths. J – Several double openings preserved on the sandstone surface, resembling *Arenicolites* and rhizoliths. K – Horizontal burrow with poorly preserved ?menisci assigned as cf. *Thalassinoides* isp.

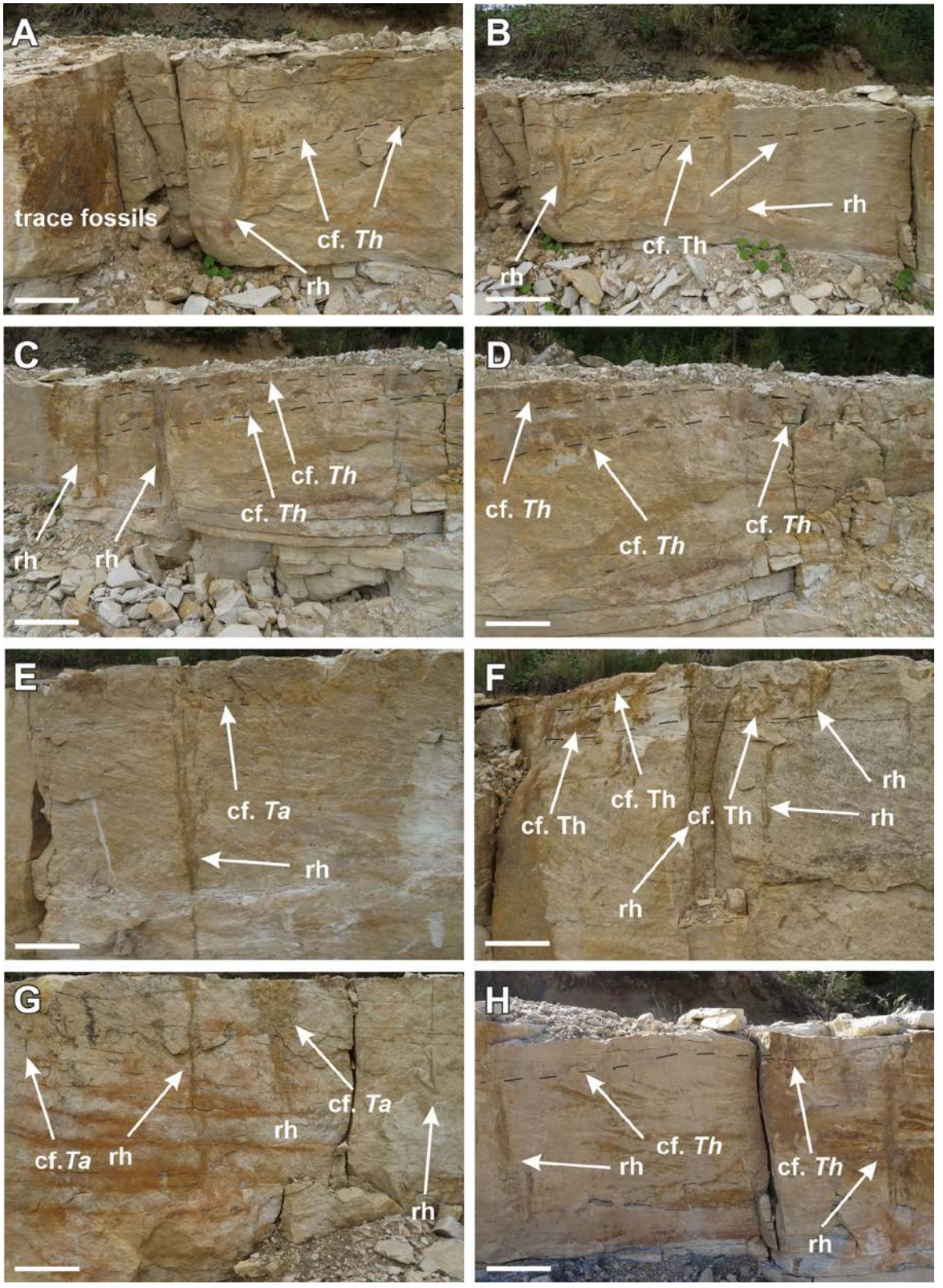

Text-fig. 11. *Thalassinoides* penetration along bedding surfaces. Abbreviations as in Text-figs 7 and 8. A–H – Trace fossil suites arranged along bedding boundaries. Trace fossils penetrated from the top beds (cf. *Thalassinoides* isp.). Some burrows assigned as cf. *Taenidium* isp. are associated with rhizoliths, which occur mostly as root casts.

Thalassinoides Ehrenberg, 1944
Thalassinoides paradoxicus Kennedy, 1967
(Text-figs 7I, 8G, 9A, D, E–G, 10A, E, K, 11A–D, F, H)

MATERIAL: Several specimens that occur at the discontinuity surface and sometimes within the yellowish sandstones. *Thalassinoides* (cf. *T. paradoxicus*) was previously reported in Krákorka Quarry by Mikuláš and Prouza (1999, pl. II/1-3), and *Thalassinoides paradoxicus* by Knaust (2021a, fig. 5F).

DESCRIPTION: Burrows appearing as interconnected, irregular cylindrical tunnels of slightly varying diameter, which represent T-shaped branching pattern and circular to elliptical cross-sections. Tunnel enlargements at the branching points are rare. The studied specimens are mostly irregularly shaped, unlined, sharp-walled, and rarely branched. Their surface is mainly smooth, without ornamentation. They are not flattened. Some blind tunnel-terminations were also present. They appear in abundance at the erosional surface, the upper boundary of the Bohdašín Formation is overlain by transgressive conglomerates of the Peruc-Koryčany Formation. Horizontal tunnels that form a burrow network prevail, though common vertical tunnels ('finger-like branches') that penetrated from this surface were also visible (Text-fig. 9A; cf. Mikuláš *et al*. 2002). The observed burrows show a constant diameter, from 1.5 to 2.5 cm, and their length varies from 10 to almost 100 cm. The dark brown – rusty color of the burrow is different from the host rock, so they are quite visible on sandstone surfaces. Some poorly preserved specimens did not show all ichnotaxobases needed for taxonomic assignment were described as cf. *Thalassinoides* (Text-figs 7I, 9D–F, 10A, K, 11A–D, F, H) or ?*Thalassinoides* (Text-fig. 9G).

REMARKS: The presence of an irregular horizontal burrow network on bedding planes connected by vertical shafts, and the occurrence of blind tunnels suggests assignment to *Thalassinoides paradoxicus* (cf. Knaust 2021b and references therein). The presence of finger-like branches pointing downwards from the discontinuity surface makes these burrows similar to the specimens described by Mikuláš *et al*. (2002), who reported *Thalassinoides* from Czech metavolcanic rocks that penetrated up to 30 cm depth (see Text-fig. 9A). The majority of studied specimens did not exhibit swellings at junctions, and so were described as cf. *Thalassinoides* (Text-fig. 9D) or ?*Thalassinoides* isp. (Text-fig. 9G). Mikuláš and Prouza (1999) recognized *Thalassinoides* (cf. *T. paradoxicus*, cf. *T. suevicus*) in Krákorka Quarry that penetrated up to 2 m below the discontinuity surface between the Bohdašín and Peruc-Koryčany Formations. However, in the present study *Thalassinoides* penetration is clearly about 30–50 cm. *Thalassinoides* might occur in the deeper part of the studied sandstones (Text-figs 7I, 10A, E, 11A–D, F, H), but the possible specimens are rare and did not show all ichnotaxobases needed for taxonomic assignment, such as swellings at junctions. They are fragmentarily preserved and represent similar branching pattern to commonly preserved rhizoliths, so discriminating these trace fossils from rhizoliths is difficult. These specimens were mostly described as cf. *Thalassinoides*. On the other hand, several authors reported the absence of swellings at *Thalassinoides* tunnel junctions (see Pervesler and Uchman 2009; Zhang *et al*. 2017; Bengtson *et al*. 2021). The morphology of some horizontal specimens that have – chevron-like menisci and walls – also slightly resembles *Beaconites* (Howard and Frey 1984; Boyd and McIlroy 2017, compare Keighley and Pickerill 1994; Text-fig. 9E). However, these diagnostic features are poorly marked, so they were also assigned as cf. *Thalassinoides*.

Thalassinoides paradoxicus is regarded as domichnia, fodinichnia, or even agrichnia (see Myrow 1995; Bromley 1996; Ekdale and Bromley 2003, respectively). It mainly characterizes the *Glossifungites* and *Cruziana* ichnofacies in firm and soft grounds (Knaust 2017, 2021b). The *Cruziana* ichnofacies is typical of shallow-marine environments, but occurs in a wide range of settings, including lagoons, bays, estuaries, and tidal flats (MacEachern *et al*. 2007; Bhattacharya *et al*. 2016; Pemberton *et al*. 2012; MacEachern and Bann 2020).

The *Thalassinoides* specimens found in the uppermost part of Krákorka Quarry are irregularly shaped, unlined, sharp-walled, and passively-filled. These features indicate excavation in a semi-consolidated, firmground substrate (cf. MacEachern *et al*. 2012). The degree of flattening in the studied *Thalasssinoides* is very low, typical of the *Glossifungites ichnofacies* (MacEachern *et al*. 2007, 2012). In this substrate-controlled ichnofacies, a low diversity trace fossil assemblage is typical, but individual burrows may be abundant (Pemberton and Gingras 2005). The associated firmground usually results from erosional exhumation of muddy or sandy compacted, dewatered, and/or early cemented substrates (Abdel-Fattah *et al*. 2016) in terrestrial, shallow-water and deep-marine settings. These firmground substrates are colonized by opportunistic tracemakers during a transgression phase, which coincides with a depositional hiatus and the

formation of discontinuity surfaces. *Glossifungites* ichnofacies suites occur in a wide range of environments, including intertidal, bay margin, brackish, estuarine, shallow marine, and deep marine settings. They are dominated by vertical and subvertical dwelling burrows of suspension-feeding organisms (*Arenicolites*) and dwelling structures of deposit feeders (*Thalassinoides*, *Taenidium*) (cf. Abdel-Fattah *et al*. 2016 and references therein). *Thalassinoides paradoxicus* is known from the Cambrian to the Recent (Mángano and Buatois 2016 and references therein).

Thalassinoides suevicus (Rieth, 1932)
(Text-fig. 9B, C, E)

MATERIAL: Several specimens preserved at the discontinuity together with numerous rhizoliths on bedding planes. *Thalassinoides* (cf. *T. suevicus*) was reported by Mikuláš and Prouza (1999, pl. II/4-4, III/1-2).

DESCRIPTION: Horizontal burrow network that consists of cylindrical horizontal tunnels with Y-shaped branching patterns. Tunnel enlargements at bifurcation points are very rare, but in some cases visible (Text-fig. 9B). The tunnel diameters vary from 1.5 cm up to 2.5 cm and the visible length is up to 40 cm.

REMARKS: The presence of horizontal specimens that mostly represent Y-shaped branching-patterns suggests assignment to *Thalasinoides suevicus* (cf. Knaust 2021a, b and references therein). However, in many cases, the studied specimens do not show the necessary ichnotaxobases for recognition and interpretation, such as enlargements of Y-shaped branchings. The invariant width at branching points makes this assignation difficult. Mikuláš and Prouza (1999, p. 336), who studied *Thalassinoides* from Krákorka Quarry, also observed that "prominent enlargements of the system at bifurcation points are rare." The *Thalassinoides suevicus* network is morphologically very similar to the rhizoliths. The similarity of the Y-shaped branching pattern produced by rhizoliths and crustaceans can be confusing (see Uchman *et al*. 2012). However, while the plant traces have similar Y-shaped branching patterns to *Thalassinoides*, they differ in having decreasing diameters.

Unrecognized trace fossils
(Text-fig. 10J)

MATERIAL: Several double openings at sandstone bedding planes. One specimen (*Arenicolites* isp.) was reported by Mikuláš and Prouza (1999, pl. I/3), 30 cm below the discontinuity surface between the Bohdašín and Peruc-Koryčany Formations.

DESCRIPTION: Some paired openings at the yellowish sandstone bedding planes. A simple U-shaped tube that is vertical or inclined to the bedding plane without spreiten is not visible. Tube diameters vary from 0.5 to 1.0 cm.

REMARKS: The presence of paired, circular traces might suggest assignment to the ichnogenus *Arenicolites* Salter, 1857. In some cases, the ichnogenus *Arenicolites* was differentiated on the basis of vertical to slightly inclined paired burrows (see Gillette *et al*. 2003), instead of the presence of U-shaped structures. However, for precise assignation polished samples of the traces are needed. Further research may be useful for precise taxonomic affiliation. At the present time, the studied specimens are left in open nomenclature.

DISCUSSION

Sedimentology of the uppermost Devět Křížů Sandstone

The sediments described here form a characteristic facies structure characterized by: (a) the repetition of three assemblages of sedimentary structures representing the lower, central and top parts of the described sediments, (b) highly bio-disturbed sediments, (c) and gravel covered levels (Text-fig. 4, sections 1–3).

We suggest that the studied quartz-kaolinitic sandstones were deposited in shallow-marine environments during the initial phase of the transgression. The presence of chamosite and glauconite confirms this interpretation (cf. Porrenga 1967; Rubio and López-Pérez 2024; Text-fig. 4, section 4). On the basis of the directions of sedimentary structures (e.g., ripple and dunes bedding, irregular wavy layering, Text-fig. 5F, G), which are directed landwards we speculate that the studied sand body represents a positive accumulation form. Furthermore, a unimodal palaeotransport direction dominates (Text-fig. 5C, E–H).

These deposits certainly cannot be considered as typical terrestrial deposits, which disregards their aeolian origin (due to the presence of common clay intralclasts) as proposed by some authors (cf. Mikuláš *et al*. 1991; Uličný 2004). Likewise, a fluvial interpretation (compare Valín 1964; Prouza *et al*. 1985; Mader 1990) is also excluded for several

reasons. First, these sediments represent an elongated (linear) morphological bedform, as opposed to a valley or river channel mesoform. If interpreted as fluvial, the presence of intraclasts and coarse material should be related with the presence of clear palaeochannels, which are not observed here (see Hiroki and Masuda 2000). Secondly, transport directions should be approximately consistent with the local palaeoslope inclination (i.e., towards the south), whereas an opposite transport direction is observed here. Third, relics of river flood plains are not preserved there, however it is not excluded that some of the clay intraclasts might have originated from the nearby penecontemporaneous floodplain, estuarine deposits or a lagoonal setting (compare Spaggiari and Bordy 2023). According to the latter authors, clasts probably were ripped up during floods and transported into the coastal setting. However, the intraclasts might be also derived from the clay covers observed in the described sediments. Beach relics are not preserved, though reactivation surfaces or storm runnel observed in the studied deposits might appear also in a beach setting (Text-fig. 6A). However, beach and coastal environments (see Holub 1972; Vejlupek 1983) seems to be completely excluded, based on the sediment transport directed to the land. Additionally, no typical tempestites are preserved (only sedimentary structures which might resemble HCS were observed; Text-fig. 6) and there is a low probability of fine-grained intraclast preservation in these high-energy environments.

The co-occurrence of gravel in the sediment, both dispersed and as residual lags, alternating with clay covers typical of suspension deposition, indicates the multi-stage, even cyclic nature of sedimentation and multi-stage sediment reworking. The studied sandstones and conglomerates are recognized herein as deposited in a spit bar setting.

Deposits from Krákorka Quarry combine sedimentary features observed in recent spit bar depositional environments, e.g., a climbing trend – a succession of several overlying cross-beds with pebble covered bases (Nielsen and Johannessen 2009; Nehyba and Roetzel 2021), reactivation surfaces with clay intraclasts, showing pseudoimbrication (Fruergaard *et al*. 2020), the presence of clay covers (up to a few centimetres) suggesting deposition from suspension during calm periods (Johanessen and Nielsen 2006; Nielsen and Johannessen 2009; Leszczyński and Nemec 2015), as well as the presence of trough cross-stratification and ripple cross lamination in the sand beds, which indicates unidirectional palaeocurrents (compare Hiroki and Masuda 2000; Table 5). The inclination of strata is low, suggesting sedimentation in shallow water (cf. Nielssen and Johannessen 2009; Leszczyński and Nemec 2015).

Therefore, the sediment structure (current ripples, wave ripples, trough cross-stratification), the hydrodynamic regime (unimodal current direction), and the depositional processes (progradation and erosion) indicate a spit bar setting (Text-figs 12, 13; Table 5).

Additionally, these controls are supported by the occurrence of clay-muddy material within the analyzed deposits. The presence of (i) sharp-edged intraclasts on the bedding surfaces (pseudoimbrication) and (ii) well-rounded, sometimes armored intraclasts, suggests there were probably two sources of the clay-muddy material. The first, 'hardened' ones were most probably derived from external sources, maybe from an adjacent lagoon area, while the second, 'fresh' intraclasts were derived directly from spit bar complex deposits. Further investigations of these differences require studies on the mineralogy of the fine-grained material from Krákorka Quarry. In this study, we have only performed pilot analyses to determine the dominant clay mineralogies, rather than a detailed, full-scale investigation.

Generally, the observed recurrent climbing associations reflect alternating accumulation and erosional conditions that are characteristic of cyclic environmental changes – from shallow to deeper water (a few to several metres) as a result of transgression, calm to high energy, and terrestrial-transitional to marine. Repeated major erosional surfaces (Text-fig. 12A) covered with gravelly sediments demonstrate that, despite the pervasive destruction of spit bars during recurrent storm events, the erosional base progressively rose and the accumulation potential was restored, resulting in spit bar development over time. Such sediment structures can only be formed in environments where progradation prevails as the dominant accumulation mechanism, and must have been accompanied by a gradual rise of the erosional base. At Krákorka Quarry, these processes are accompanied by the zonation of sediment settlement and penetration by both invertebrate trace fossils (*Thalassinoides*, cf. *Taenidium*) and vegetation, including trees (rhizoliths; see trace fossils suites arranged along bedding boundaries in Text-figs 6C, 11, 12). However, it seems that penetration by both marine invertebrate trace makers of *Thalassinoides* isp. and terrestrial producers of *Taenidium* isp. along the bedding surfaces, took place after exposure of the described sediments rather than contemporaneously with deposition (see above, Text-fig. 14). Collectively,

	Physical sedimentary features																														Processes and environments											
	physical textures (grain size)							litho-logy		primary sedimentary structures											deforma-tions			biogenic								processes					transport			environmet		
data source (chronologically)	1	2	3	4	5	6	7	8	9	10	11	12	13	14	15	16	17	18	19	20	21	22	23	24	25	26	27	28	29	30	31	32	33	34	35	36	37	38	39	40	41	42
Nielsen *et al*. (1988)	+	+	+		+	+		+		+	+	+	+	+	+	+	+	+	+	+	+		+		+						+	+	+	+	+	+		+	+	+	
Rasmussen and Dybkjær (2005)	+	+	+					+	+						+		+	+	+						+	+				+		+	+	+	+	+				+		+
Lindhorst *et al.* (2008)										+			+		+				+	+											+		+	+	+							
Shukla *et al*. (2008)		+	+									+	+	+	+	+		+	+														+	+						+	
Rasmussen *et al.* (2010)		+	+			+		+	+	+	+				+									+	+				+		+	+	+		+		+				
Reimann *et al.* (2012)	+	+	+		+				+						+			+	+																	+				+		
Tillmann and Wunderlich (2013)		+	+			+	+								+	+		+	+					+		+	+				+	+	+	+					+		
Billy *et al.* (2014)	+	+	+		+	+					+				+			+													+			+						+	+
Clemmensen *et al.* (2014)		+	+	+	+	+												+								+			+		+				+	+				+	
Tillmann and Wunderlich (2014)	+	+	+	+	+	+	+											+								+			+			+			+					+		
Nehyba and Roetzel (2021)	+	+	+	+	+	+		+	+	+	+		+	+	+	+		+					+		+						+	+			+	+					+
Shawler *et al.* (2021)	+	+	+												+	+			+	+						+				+	+	+	+		+							+
Pellerin Le Bas *et al.* (2022)		+	+																													+	+		+							
Spaggiari and Bordy (2023)	+	+	+	+	+	+	+	+							+	+		+	+	+		+			+	+	+		+		+	+	+	+	+	+	+		+		+
Chrząstek and Wojewoda (this paper)	+	+	+		+	+		+	+	+	+	+	+	+	+	+		+	+							+	+	+	+	+	+	+		+	+	+					+

Table 5. Characteristic features of spit bar systems, based on Nielsen *et al.* (1988), Rasmussen and Dybkjær (2005), Lindhorst *et al*. (2008), Shukla *et al*. (2008), Rasmussen *et al*. (2010), Tillman and Wunderlich (2011, 2013), Reiman *et al*. (2012), Billy *et al*. (2014), Clemmensen *et al*. (2014), Nehyba and Roetzel (2021), Pellerin Le Bas *et al*. (2022), Shawler *et al.* (2021), and Spaggiari and Bordy (2023). 1 – clay; 2 – silt (mud); 3 – sand; 4 – granule; 5 – gravel; 6 – pebble; 7 – cobble; 8 – clay intercalations; 9 – clay intraclasts; 10 – current ripples; 11 – wave ripples; 12 – ripple cross-lamination; 13 – dune cross-bedding; 14 – trough cross-bedding; 15 – low angle cross-bedding; 16 – large scale foreset cross-bedding; 17 – hummocky cross-bedding (HCS?); 18 – reactivation surfaces; 19 – channel; 20 – rip current channel; 21 – water escape (dewatering) structure; 22 – desiccation cracks; 23 – slump contortions and folds; 24 – fossil fauna; 25 – trace fossils; 26 – root casts; 27 – rhizocretions; 28 – rhizoliths; 29 – paleosol; 30 – fossil trunks; 31 – vegetation; 32 – waves; 33 – longshore currents; 34 – tides; 35 – storms; 36 – transgression; 37 – unidirectional current; 38 – bidirectional current; 39 – transverse current; 40 – tidal delta; 41 – beach setting; 42 – lagoon setting.

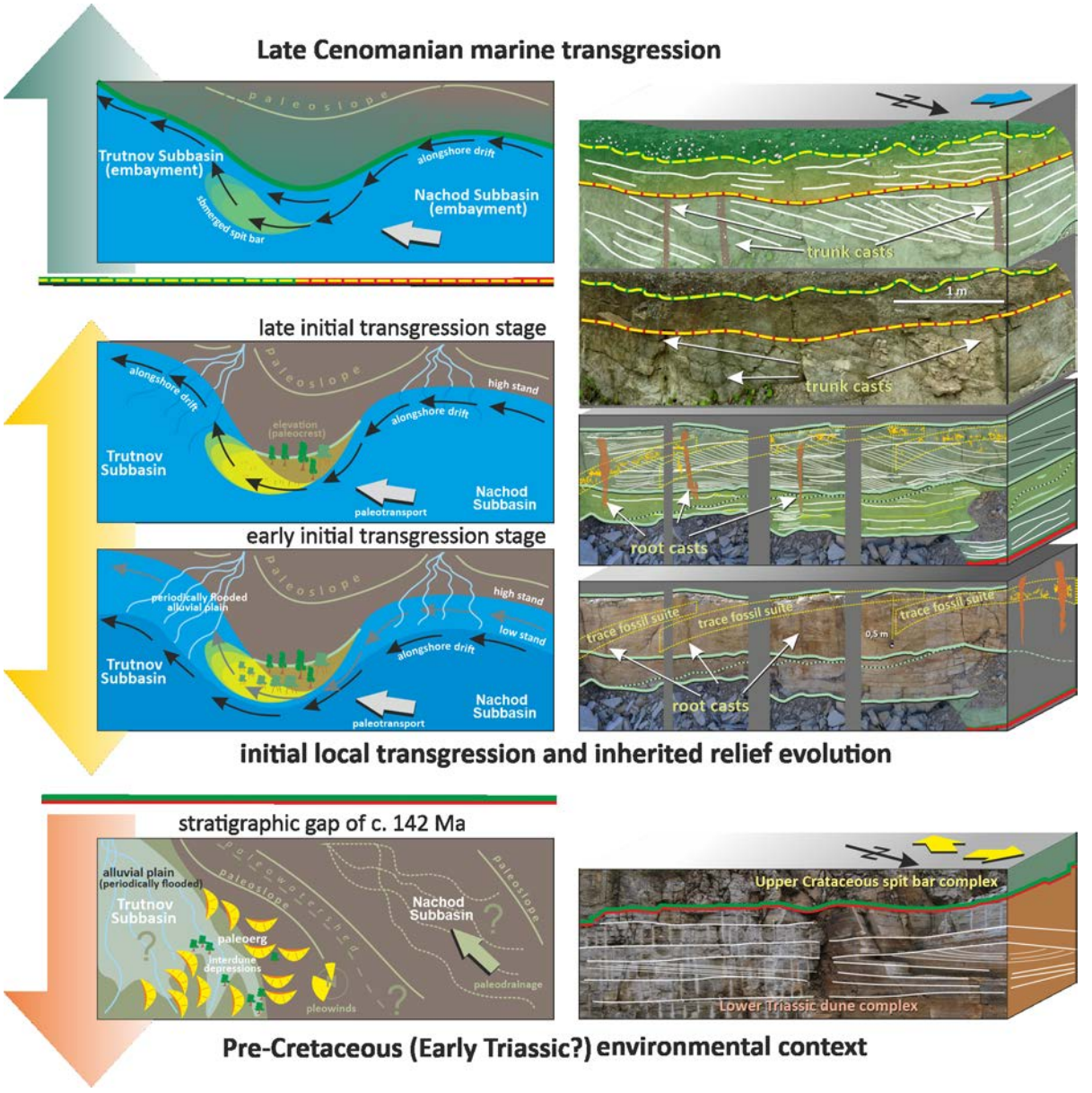

Text-fig. 12. Four main stages of palaeogeographic development in Krákorka (left) and related facies associations (right).

these controls point to a transitional palaeoenvironment during progressive sea level rise and associated transgression.

Thus, we suggest that these sediments are (i) distinct from the underlying portions of the Bohdašin Formation, and (ii) link them with the regional Late Cretaceous transgression. The topographic conditions preceding the transgression could conceivably stimulate the formation of local accumulation zones within the inherited bathymetric relief – that is, a palimpsest. In this framework, progressive relative sea level rise successively removed individual localities from the direct local impact of coastal abrasion and accumulation, thus unifying the facies assemblages within the marine basin.

In summary, only a spit bar depositional environment can feasibly explain all of the phenomena in Krákorka Quarry, including the cuspate shape of a spit bar, which usually arises in the final phase of spit bar development, explaining the clearly-recorded progradation of the accumulation form ‘up the paleoslope’ (cf. Text-fig. 13). We postulate a model of a

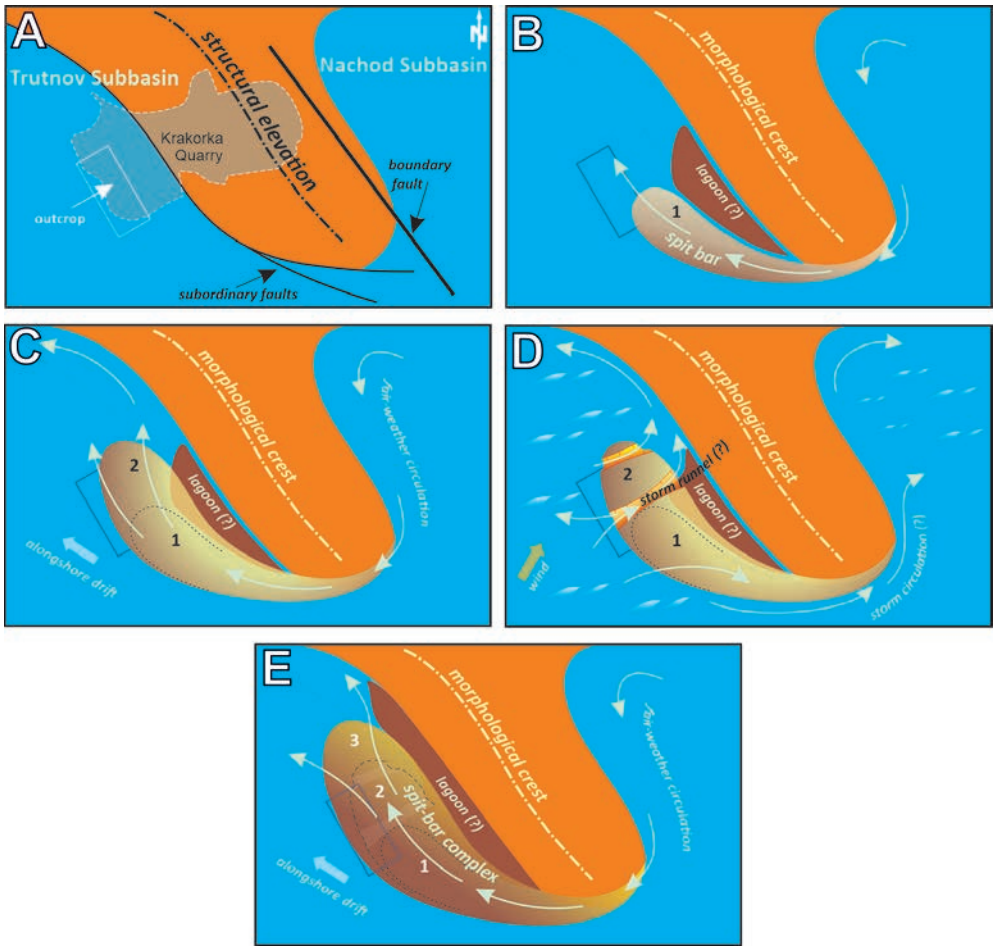

Text-fig. 13. Diagram showing spit bar system development during the initial Late Cretaceous marine transgression. Local topography inherited from the pre-transgressive period, most likely related to synsedimentary tectonic activity that influenced the location depositional loci in the Sudetic sedimentary basins (A); subsequent stages of spit bar development (B, C and D), and the initial development of a regional transgressive sequence (E).

recurved ('hacked') spit after King and Mc Cullagh (1971) and Ashton *et al*. (2007), in which "spits also recurve, or trend back towards the shore-even the high-energy, seaward-facing side of a spit faces many directions, experiencing waves from a variety of deep-water directions" (cf. Ashton *et al*. 2007, p. 352).

We suggest that the uppermost Devět Křížů Sandstone was deposited during the middle or early late Cenomanian transgressive phases, before the main latest Cenomanian–early Turonian transgression. This insight may be useful for slightly altering the northern Bohemian Late Cretaceous palaeogeography, with the seashore located c. 30 km north of the study area and NWW to SEE-oriented (cf. Jerzykiewicz and Wojewoda 1986).

It cannot be excluded that the Krákorka deposits were initially deposited in the Jurassic; Valečka (2019), however, reported that erosion and peneplanation removed Jurassic deposits from the northwestern and central Bohemian Massif during the Early Cretaceous, leaving only small relic deposits in northern Bohemia, Saxony, and Brno area. The unique nature of the study area, which was already a morphological elevation at the junction of the Trutnov and Náchod subbasins in the Triassic, suggests that Jurassic deposition was unlikely.

The Náchod and Trutnov subbasins, together with the Mnichovo-Hradišče and Kudowa subbasins that collectively form the Intra-Sudetic Basin Suite, show many features typical of pull-apart basins and collectively form one of the most significant, long-lived (Carboniferous to Recent?) tectonic zones in the northern periphery of the Bohemian Massif – the Intra-Sudetic Shear Zone (Wojewoda 2007a).

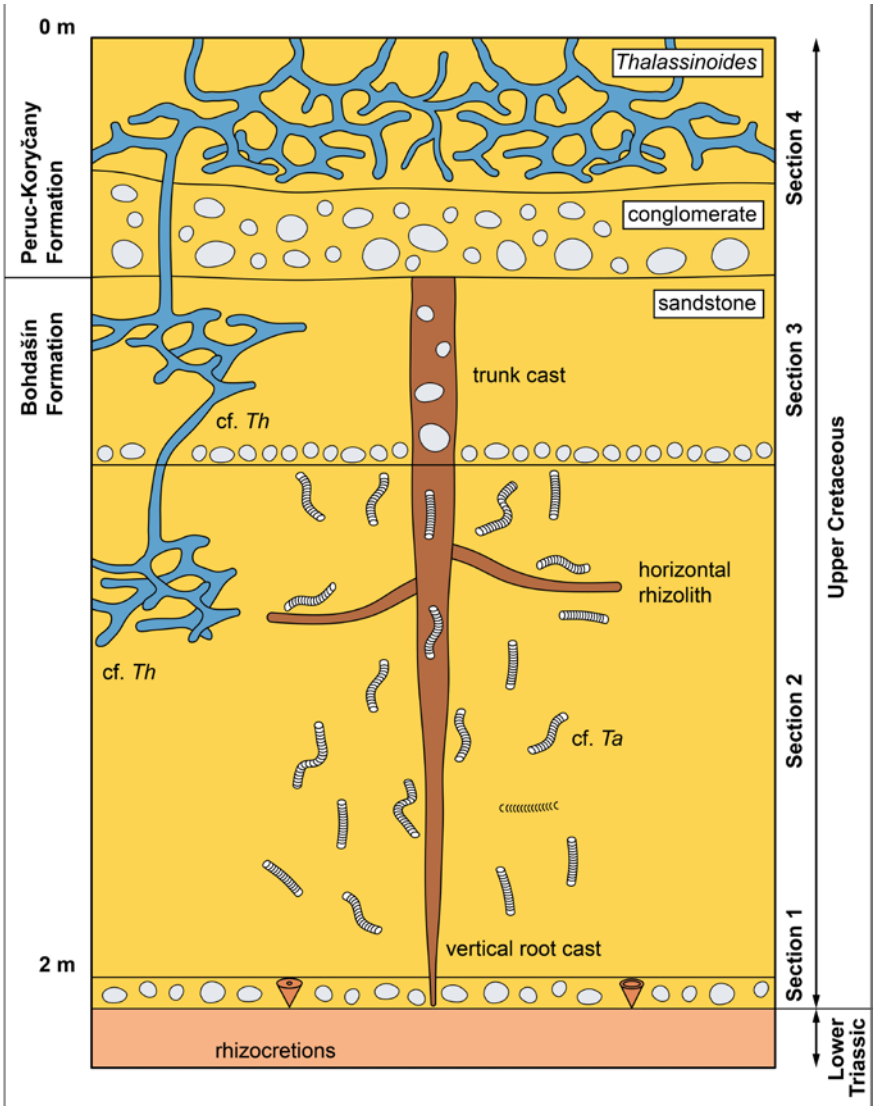

Text-fig. 14. Diagram of distribution of trace fossils in sandstones and conglomerates of the uppermost Devět Křížů Sandstone, modified after Bromey and Ekdale (1986) and D'Alessandro *et al*. (1993). Abbreviations as in Text-figs 7 and 8; explanations of individual sections (1–4) as in Text-fig. 4.

The northern boundary of this zone is the Poříčí-Hronov Fault Zone, which bounds the Intra-Sudetic Synclinorium from the south (Mencl *et al*. 2013; Wojewoda *et al*. 2016). It is worth emphasizing that the northern frame faults of the Poříčí-Hronov Zone were repeatedly reactivated and played a significant role in shaping the regional palaeogeography during the Permian, Triassic, and Cretaceous (cf. Teisseyre 1968, 1973, 1975; Teisseyre and Teisseyre 1969; Jerzykiewicz and Wojewoda 1986; Uličný 2001, 2004; Uličný *et al*. 2003, 2009; Text-figs 2A, 3–5). The geodynamic and palaeogeographic context has been previously extensively discussed (cf. Wojewoda 1986, 2007a, b, c, 2009; Wojewoda and Kowalski 2016; Wojewoda *et al*. 2016, 2022), and we refer the reader to those publications for further details. For our purposes, it suffices to note that the boundary faults of the Náchod and Trutnov subbasins probably played a particularly important role in shaping the palaeotopography of this area. The fossil pit bar system clearly relates to the course of one such fault (Text-fig. 2A).

The fossil spit bar deposit described in Krákorka is unique, if only because it was preserved in a place that was already a morphological elevation in the Triassic (cf. Wojewoda *et al*. 2016, 2022). Transgression most

often results in the levelling of the underlying terrain, enabling the deposition of a classic transgressive sequence, but in this situation the spit system development was uniquely associated with the inherited relief. 142 Myr earlier, a series of aeolian deposits had been formed and preserved in this locality (Text-figs 2A, 4). The presence of anomalously abundant tectonic phenomena, including syn-sedimentary features, in both Triassic and Cretaceous sediments (Wojewoda *et al*. 2016) is also unique in the context of the Intra-Sudetic basins (cf. Text-figs 2, 3).

In summary, it is worth observing that the uppermost Devět Křížů Sandstone does not correspond to the palaeoenvironmental and palaeogeographical realities of the Early/Middle Triassic in Central Europe, excluding the possibility of associating the studied deposits with either the majority of the Devět Křížů Sandstones in Krákorka or with the broader Bohdašín Formation. Instead, we find it more useful to compare these deposits with a transgressional Upper Cretaceous sequence.

Spit bar systems

Spit bars actively develop in a diversity of fresh-, transitional-, and marine environments (e.g., Krist and Schaetzl 2001; Jewell 2007; Schaetzl *et al*. 2016; Lopez 2022). They most often appear where there is excess sediment influx: for example, (1) close to river mouths, (2) where both along-shore drift and waves are influential depositional controls, and (3) in association with gradual water level, all conditions favourable for transgressional deposition. Sometimes shoreline peculiarities, such as headlands or clearly indented bays, drive the development of spit bars.

It is difficult to directly examine the internal structure of Recent spit bar systems, due to sediment waterlogging and/or subaqueous retention. Localities in which these systems can be directly described are unique. Some sub-fossil spit bars have revealed internal structures in natural outcrops, in basins where locally or regionally sea-level evolution has transitioned from transgressive to regressive (e.g., Lopez 2022; Spaggiari and Bordy 2023).

Scientifing understanding of the internal structure and architecture of spit bar sediments dramatically benefited from the introduction of high-resolution seismic methods (e.g., Novak and Pedersen 2000; Lobo *et al*. 2003, 2005), and ground penetration radar (GPR) in geophysical prospecting, defining 'GPR structural facies' and associated sedimentological interpretations (e.g., Daly *et al*. 2002; Jol *et al*. 2002; Neal 2004; Shukla *et al*. 2008; Craig *et al*. 2012). Remote mapping methods have also proved important for recognizing the contemporary development of spit bars, in particular high-resolution LIDAR digital terrain models (e.g., Taveneau *et al*. 2021; Pancrazzi 2022) and photogrammetry (e.g., Simeoni *et al*. 2007; Rodriguez-Santalla and Somoza 2018, Robin *et al*. 2020; Rodriguez-Santalla *et al*. 2021). Additional information about the bathymetry of spit bar systems has been revealed through the use of multi-beam sonars (cf. Shaw *et al*. 2019). However, older maps have provided equally insightful understanding into the historic dynamics of spit bars, especially once processed by topological calibration (H-GIS) (e.g., Boer and Carr 1969; Panin and Overmars 2012; Somoza and Rodríguez-Santalla 2014; Gupta and Rajani 2020).

Recent spit systems may constitute very large elongated and mostly sandy-gravel bodies. For example, the best known Holocene-to-Recent spit system, the Danish Skagen, is 22 km long, 3–7 km wide, and up to 32 m thick, and dominantly consists of cross-bedded sand deposited under c. 0.3–9.5 m water depths (Johannessen and Nielsen 2006).

However, within the recognized contemporary or sub-fossil coastal systems, spit bar formations are relatively thin, from 2 to c. 10 m, and occur within a predictable Waltherian position – that is directly above terrestrial environments (e.g., alluvial, deltaic), in association with marine sediments (initial transgressive deposits), and below the main transgressive marine sediments, which usually form a transgressive sequence that almost always begins with a transgressional boulder lag (e.g., Lindhorst *et al*. 2008, 2010; Reimann *et al*. 2012; Flemming and Martin 2021).

Contemporary spit bar sediments are texturally very diverse. Sediment grain sizes and petrography are determined by the type of supplied material, which in turn is determined primarily by the geological structure, size, and geomorphology of the associated river catchment. Of course, the material deposited on upper spit bar surfaces largely acquires features dependent on the dominant marine processes – that is, the coastal current and wave system. The distance from the sediment source to the depositional site also has influence on the sediment texture.

As such, spit bar sediments may form heterolytic systems, which are prevalent in modern mid-latitudes. But they can also be sandy or gravelly systems, which tend to be more common in sub-polar zones. Sedimentary analyses of contemporary spit bar sediments are easier to perform than fossil spit bars, because they do not require intact sediment structures, so they can be taken from depth by drilling (e.g., Ollerhead and Davidson-Arnott 1995; Costas

and Fitzgerald 2011; Peterson *et al*. 2011; Janušaite *et al*. 2022, 2023).

Modern active or sub-fossil spit bars have very well understood internal structures. To date, palaeohydrodynamic indicators suggest that spit bars capture almost all possible sediment transport directions relative to shoreline orientations. There are several potential reasons for this unusual situation. First, the frontal growth (progradation) of individual spit bars is not linear, but often changes in direction. Secondly, a spit bar is usually not a single bedform, but instead often composes a compound system resulting in the formation of a spit bar complex (cf. Clemmensen *et al*. 2014). Third, during transgression, the relative location and shape of the shoreline is constantly modified, resulting in forced evolution of the spit bar system.

At the same time, spit bars are the only known modern coastal system in which both the macroform and current forms (ripples and dunes) migrate towards land, leading to a long-lived, consistent aggradation of the spit bar system. Periodic transverse cutting of the spit bar system during storms, periodic ascent, and/or vegetative overgrowth of the spit bar does not change this tendency until the spit bar is ultimately buried and fossilized (for instance, by being covered by transgressive sediments; e.g., Nielsen *et al*. 1988; Allard *et al*. 2008; Pancrazzi *et al*. 2022; Spaggiari and Bordy 2023). Almost all workers of contemporary and/or subfossil spit bar systems emphasize that the appearance, development and/or preservation of sediments in these systems is contingent upon constant sea level rise, that is, in a regional transgressive regime (cf. Christiansen *et al*. 2004; Johannessen and Nielsen 2006).

While modern or sub-fossil spit bar systems are quite common, descriptions of geologic structures with features analogous to Recent spit bars are relatively infrequent. It is difficult to assess whether this is due to the low frequency and dissemination of actualistic research among sedimentary geologists, or because of the unusual environmental and basin conditions that can lead to the fossilization of such systems. After all, a spit environment is not as ephemeral as, for example, an aeolian dune environment. That being said, the lifetime of a spit bar is several orders of magnitude shorter than that of an equivalent transgressive sediment complex. Perhaps, therefore, this discrepancy may result from the rate of marine transgression, which may be difficult to determine in older formations due to difficulties in temporally resolving these distinct environmental systems.

The oldest interpreted fossil spit bar deposits are from the Upper Jurassic Sognefjord Formation (Troll West Field, Norwegian shelf; Dreyer *et al*. 2005; Nehyba and Roetzel 2021). Several spit bar formations have been documented in Cretaceous strata. Johannessen and Nielsen (2009) presented the possibility of using the spit bar model for the Upper Cretaceous Shannon Sandstone (Western Interior Seaway, USA). Subsequently, Merletti *et al*. (2018) interpreted 15 rock bodies as 'Bar Spit Units' within the upper Campanian to Maastrichtian Almond Formation (Wyoming, USA), which had average sizes of 6–12 m estimated lifetimes of 20 kyrs. Rasmussen and Dybkjær (2005) similarly interpreted selected sandstone bodies from the upper Oligocene and lower Miocene of Eastern Jylland (Denmark). Finally, a very detailed sedimentological analysis of the Miocene Burgschleinitz Formation (Austria) suggested that it is most parsimoniously interpreted as a spit bar system deposit (Nehyba and Roetzel 2021). It is worth mentioning that these sediments reach a maximum thickness of about 6 m, and are overlain by clearly transgressive sediments.

Paleosol characteristics

The existence of rhizoliths in the studied sandstones may suggest that they should be regarded as paleosols (cf. Rettalack 2001). The preservation of root traces in the deposit should have induced physical and chemical changes in the host rock (Badawy 2018). However, initial soil development was only noticed in the studied rhizolith-bearing horizon. Genise *et al*. (2004) postulated that some paleosols show well-developed pedofabrics without preserved trace fossils, while others may be intensely bioturbated but without changes in soil character. Esperante *et al*. (2021) reported the occurrence of rhizoliths from a variety of depositional settings, including loess, and sandy eolian, lake margin, coastal plain, marginal marine, and alluvial deposits. Buynevich *et al*. (2007) suggested that four paleosol horizons were present in a 30–40 m deep sequence, resulting from a barrier-spit facies. Moreover, well-developed paleosols may contain a higher density of long root casts (up to 2 m in length), indicating a seasonally dry environment (cf. Nascimento *et al*. 2019), as in the studied deposits. There are numerous examples of root penetration in weakly lithified or even hard substrates (Uchman *et al*. 2012). Deep roots could penetrate deposits up to 3.5 m deep (cf. D'Alessandro *et al*. 1993); similar depths of penetration, ranging from 1 m up to 4–5 m, although most commonly from 1–2 m were postulated by other authors (Plaziat and Mahmoudi 1990; Uchman *et al*. 2012; Esperante *et al*. 2021; Hsieh and Uchman 2023; Nascimento *et al*. 2023).

Mikuláš and Prouza (1999), who first described root traces in the Krákorka Quarry, suggested that they may result from a marginal marine ?mangrove swamp. Mangrove forests are very common along tropical and subtropical shores (Srikanth *et al*. 2015). Importantly, living or fossil mangrove roots are characteristically associated with marine bioturbation, such as the ichnofossils *Ophiomorpha*, *Thalassinoides*, *Palaeophycus*, *Skolithos*, and *Taenidium* (Gregory *et al*. 2004; Abdel-Fattah and Gingras 2020). Additionally, bivalves, gastropods, scaphopods, arthropods, and vertebrate body fossils commonly occur in such deposits (cf. Abdel-Fattah and Gingras 2020). The latter authors reported the predominance of *Thalassinoides suevicus* in an upper middle Eocene shallow-marine lagoon that shoaled into a bay margin environment with mangroves. The earliest fossil-mangrove ecosystem is known from the Late Cretaceous, but mangroves became globally abundant in the Eocene to Miocene (Srivastava and Prasad 2019). Badawy (2018) reported mangrove rhizoliths from Oligocene fluvio-marine deposits, which were assigned to a tropical and/or subtropical rain forest environment. A mangrove origin of the rhizoliths in Krákorka Quarry associated with bay-margin or lagoon settings under brackish to marine salinity seems to be possible (compare Basyuni *et al*. 2007), although the existence of other vascular plants cannot be excluded. On the other hand, body fossils are absent from Krákorka Quarry aside from a single internal mold of an indeterminate bivalve found during fieldwork, despite the usual abundance of body fossils in mangrove swamps. Moreover, it is very difficult to distinguish between bioturbation by marine and terrestrial invertebrates in paleosol settings due to their morphological similarity (cf. Berry and Staub 1993; D'Alessandro *et al*. 1993; Gregory *et al*. 2004; King *et al*. 2021). However, the *Taenidium* ichnofabric, which appears in the study deposits, is common in ancient paleosols (see above; Nascimento *et al*. 2019, 2023). *Taenidium barretti* and *T. serpentinum* are the most abundant ichnotaxa in such settings. The close relationship between the invertebrate traces and rhizoliths may suggest that the *Taenidium* tracemaker was a non-marine animal, for instance an insect or insect larvae that colonized subaerially exposed surfaces (cf. D'Alessandro *et al*. 1993; Gowland *et al*. 2018). Moreover, *Thalassinoides* bioturbation might have occurred during the late Cenomanian transgression, after prolonged emergence. In the model of the recurved spit bar presented here (Text-fig. 13), the formation of a lagoonal setting with mangrove vegetation seems to be possible. Therefore, the mangrove swamp origin of the rhizoliths, which were observed in the studied deposits, cannot be excluded.

Ichnological analysis

In Krákorka Quarry, a low diversity trace fossil assemblage comprising *Thalassinoides paradoxicus*, *T. suevicus*, *Thalassinoides* isp., cf. *Thalassinoides* and cf. *Taenidium* was observed (Text-figs 7I, J, 8E, G, 9–11). Ichnological analysis suggests that two discrete trace fossil assemblages are present: the cf. *Taenidium* suite and the *Thalassinoides* suite (Text-fig. 14). The *Thalassinoides* suite dominates at the erosional surface between the Bohdašín Formation and the overlying Peruc-Koryčany Formation (Text-figs 4, 5H, 14). The *Taenidium* suite is usually associated with rhizoliths, which are the most common biogenic structures within the studied sandstones. The percentage of substrate (bedding planes; BI) after Miller and Smail (1997) affected by burrowing was mainly measured for *Thalassinoides* assemblages, while the vertical disturbance of original bedding (ii) after Droser and Bottjer (1986) was quantified for both the cf. *Taenidium* and *Thalassinoides* assemblages.

cf. Taenidium *suite*

The cf. *Taenidium* burrows are arranged along both horizontal and vertical rhizoliths (Text-fig. 10B–D, F–I). They are mostly vertical or inclined in relation to bedding planes. The burrows are mainly similar to *Taenidium barretti* Bradshaw, 1981, and in some cases to *T. serpentinum* Heer, 1887. Trace fossils (cf. *Taenidium*) appear in abundance in close vicinity to roots, while they are less numerous at a distance from the root casts (compare Hsieh and Uchman 2023; Text-fig. 10A–D, G, H). A cross-cutting pattern caused by overlap is commonly observed in the cf. *Taenidium* suite (Text-fig. 10A, G). Approximately 30–50 burrows were observed per 0.5 m^2 in the vicinity of root casts and horizontal rhizoliths. The ichnofabric indices (cf. Droser and Bottjer 1986) in the *Taenidium*-bearing sandstone were ii = 3–4, indicative of moderately to highly bioturbated deposits.

The current deposits show some affinities in burrowing style to other rhizolith-bearing horizons from ancient paleosols reported by D'Alessandro *et al*. (1993), Knaust (2015), Mineiro *et al*. (2017), Mineiro and Santucci (2018), Hsieh and Uchman (2023) and Nascimento *et al*. (2023). These authors

reported a *Taenidium* ichnofabric produced by insects and associated with rhizoliths, with burrows that might overlap the roots or clustered tightly around the plant traces (see D'Alessandro *et al*. 1993; Hsieh and Uchman 2023). Nascimento *et al*. (2023) postulated that extant beetle larvae populations could generate up to 70 burrows per 1 m^2 of soil and extend down to over 1 m. More burrows were observed in the uppermost studied paleosol. This phenomenon may be linked with the rapid exploration of the sediment by insects during 'intrusion time', as suggested by Gingras *et al*. (2008) and Hsieh *et al*. (2023). When insect tracemakers settle in a deposit, locomotion rates subsequently slow ('subsequent time', cf. Gingras *et al*. 2008). The moderate-to-highly bioturbated deposits might indicate the presence of opportunistic trace-makers bioturbating during episodically favourable conditions. It might suggest colonization by terrestrial trace-makers during the 'short-colonization window', an interval during which organisms are able to colonize a trace fossil-preserving substrate (cf. Nascimento *et al*. 2023 and references therein), perhaps during subaerial exposure. Gregory *et al*. (2004) also postulated that a moist root-protected environment was a desirable microhabitat for a number of invertebrates that occupy the vadose zone (see Smith *et al*. 2008, fig. 7), a point reiterated by numerous authors, including Retallack (1976, 1988), D'Alessandro *et al*. (1993), Gregory *et al*. (2004), Hsieh *et al*. (2023) and Nascimento *et al*. (2023).

Roots provide food and shelter for many invertebrates (Hsieh and Uchman 2023). On the basis of ichnological studies, many authors described insect traces in close vicinity to roots, suggesting commensalism, parasitism, mutualism, symbiosis, or other interactions (see discussion in Hsieh and Uchman 2023). Insects, such as beetles or cicada nymphs, eating or colonizing roots in the geologic record were postulated by Krause *et al*. (2008), Knaust (2015), Genise (2016, 2019), and Nascimento *et al*. (2019). Commensalism was proposed by D'Alessandro *et al*. (1993), who suggested bacterial presence around roots. However, in many cases insects consume roots, which is suggestive of parasitism (see Gregory *et al*. 2004; Krause *et al*. 2008; Genise 2016). Trace fossil occurrence adjacent to roots may be associated with less resistant deposits, which could facilitate burrowing (cf. Hsieh *et al*. 2023). Furthermore, Hsieh *et al*. (2023) postulated that after the roots are dead, other inhabitants may feed on the residual organic matter and utilize empty spaces. In summary, the abundance of possible insect traces (cf. *Taenidium*) in close vicinity to roots or arranged along horizontal rhizoliths is evidence of invertebrate-plant interactions (Text-fig. 10A, B, D, G, H). Furthermore, Mikuláš and Prouza (1999) suggested that the root canals might be later colonized by other squatters.

The studied *Taenidium* assemblage is characteristic of the *Scoyenia* ichnofacies, which occurs in low-energy, periodically exposed subaqueous deposits or periodically flooded subaerial sediments, both indicative of a transitional aquatic and terrestrial environment (cf. MacEachern *et al*. 2012; Sedorko *et al*. 2020). The low ichnodiversity but high abundance of individual trace fossils is indeed supportive of this premise. In the *Coprinisphaera* ichnofacies, by contrast, ichnodiversity is usually moderate to high and bioturbated deposits are permanently subaerially exposed (cf. MacEachern *et al*. 2012).

Monotypic *Taenidium* ichnofabrics have been commonly described from abandoned channels or floodplains in Cretaceous paleosols (cf. Nascimento *et al*. 2023). The *Taenidium barreti* ichnofabric and rhizoliths occur on the top of bars, channels, and crevasse splays under more moist conditions, allowing vegetation to persist. A marginal marine setting with a vegetal cover, periodically submerged and bioturbated by terrestrial tracemakers, seems to be the most likely palaeonvironment for the Krákorka Quarry. Bioturbation of the cf. *Taenidium* suite might have occurred during episodic subaerial exposure of the spit bar deposit. During emergence, the spit bar was presumably overgrown by vascular plants (?mangrove roots) and later burrowed by terrestrial insects.

Thalassinoides *suite*

In Krákorka Quarry, *Thalassinoides suevicus* was mainly recognized on horizontal bedding planes (Text-fig. 9B, C, E), such as the discontinuity surface between the Bohdašín and Peruc-Koryčany Formations, whereas *Thalassinoides paradoxicus* or cf. *Thalassinoides* isp. prevailed on the vertical surfaces (Text-fig. 9A, D). However, the latter ichnotaxon also occurs on horizontal bedding planes (Text-fig. 9E, F). Clear vertical occurrences of *Thalassinoides* extend up to 30–50 cm below the discontinuity surface (Text-figs 6C, 9A, D). While it cannot be excluded that *Thalassinoides* might occur deeper in the studied sandstones, for instance up to 1.5–2 m deep as suggested by Mikuláš and Prouza (1999) (Text-figs 7I, 10E, 11A–D, F, H), these specimens are fragmentarily preserved, did not show the ichnotaxobases needed for their assignment,

and so were mostly described as cf. *Thalassinoides*. However, Mikuláš and Prouza (1999) reported that "bioturbation intensity increases towards the top of the formation, reaching the base of the weakly lithified oligomictic glauconitic conglomerates of the lowermost Peruc-Koryčany Formation" (cf. Mikuláš and Prouza 1999, p. 336, pl. I, fig. 2).

Bedding-plane surfaces were moderately to highly affected by *Thalassinoides*. As in the *Taenidium* suite, the ichnofabric indices (ii = 3–4) were indicative of moderate to high bioturbation in the *Thalassinoides* suite. The presence of abundant *Thalassinoides paradoxicus* and *T. suevicus* at the erosional surface between the Bohdašín and Peruc-Koryčany Formations (Text-figs 4, 5G, 9A–E) may suggest the *Glossifungites* ichnofacies, which is characteristic of firm, unlithified substrates and often demarcates discontinuity surfaces along a depositional hiatus (cf. Gingras *et al*. 2002; Abdel-Fattah *et al*. 2010, 2016; Knaust 2021a, b). The colonization of discontinuity surfaces usually requires marine conditions and corresponds to transgressive intervals (Abdel-Fattah *et al*. 2016), however, an example from fluvial deposits was also reported (see Fürsich and Mayr 1981). In general, well-developed *Glossifungites* ichnofacies suites (cf. MacEachern *et al*. 1992) show high bioturbation intensities, a low to moderate trace fossil diversity, and large burrow penetration up to 2 m deep in muddy and sandy deposits.

There are numerous examples of *Thalassinoides* burrow penetration into semi-lithified or weathered substrates. Korneisel *et al*. (2015) and Bengtson *et al*. (2021) described a complete burrow system of Eocene *Thalassinoides* and *Taenidium* that penetrated the uppermost 5 cm of Proterozoic metaquartzites (1.7 Ga), which were loosened by weathering. Bengtson *et al*. (2021) compared this penetration with the invasion of Cretaceous *Thalassinoides* tracemakers into the weakly lithified Devět Křížů Sandstone and weathered metavolcanic rock in northern Bohemia (see Mikuláš and Prouza 1999 and Mikuláš *et al*. 2002, respectively). Gingras *et al*. (2002) reported that *Thalassinoides* descended up to 80 cm below the erosional surface, Abdel-Fattah *et al*. (2016) – up to 2 m below, Foster *et al*. (2020) – up to 60 cm below, and Mikuláš *et al*. (2002) – up to 30 cm below.

The firmground in the topmost yellowish quartz sandstones and conglomerates seems to be allogenic (cf. Abdel-Fattah *et al*. 2016 and references therein). Allogenic expressions of the *Glossifungites* ichnofacies are strongly related to eustasy and associated with transgressive surfaces, maximum flooding surfaces and/or flooding surfaces. They are characterized by low ichnodiversity and moderate to high bioturbation intensity (BI = 3–5). The current *Thalassinodes* assemblage shows little or no compaction and deep burrow penetration up to 50 cm, and in some cases even to 1–2 m (compare Abdel-Fattah *et al*. 2016, fig. 10C). The current deposits capture moderate to high bioturbation, with a dominance of deposit feeders (*Thalassinoides*) with subordinate domichnia, e.g., *Arenicolites* (cf. Mikuláš and Prouza 1999). The burrow penetration suggests an allogenic expression of the *Glossifungites* ichnofacies (compare Abdel-Fattah *et al*. 2016). Abdel-Fattah *et al*. (2016) reported flooding surfaces from Egyptian middle to upper Eocene deposits that were mainly characterized by large *Thalassinoides* up to 2–5 cm in diameter and subordinate *Arenicolites*. They suggested that the large diameter of *Thalassinoides* is consistent with low-moderate energy conditions in well-oxygenated, nutrient-rich sediments. Similarly, Villegas-Martin *et al*. (2020) suggested that the presence of large burrows in association with allogenic surfaces is a potential firmground signature. The burrow tracemakers, mainly thalassinid crustaceans, were the primary colonizers and probably had sufficient time to explore the exhumed substrates.

Marine crustacean bioturbation took place during the main phase of the late Cenomanian transgression. It should be noted that the *Thalassinoides* tracemakers used the sedimentary bedding surfaces (layering surfaces) when penetrating into the studied deposits during the main phase of the late Cenomanian transgression (see Text-fig. 11A–D, F, H). Mikuláš and Prouza (1999) suggested that the Devět Křížů Sandstone might have formed the Cenomanian seafloor. They further noted that all *Thalassinoides* tunnels were opened on the erosional surface between the Bohdašín and Peruc-Koryčany Formations, and their fill contains glauconite. Uličný (2004) also suggested that bioturbation of the Devět Křížů Sandstone was undoubtedly attributable to Cenomanian marine organisms.

It is not possible to ascertain if syn-depositional burrowing occurred based on the studied trace fossil assemblages. However, some horizontal burrows assigned to cf. *Thalassinoides* (Text-fig. 10K) might suggest such a burrowing style. D'Alessandro *et al.* (1993) reported *Thalassinoides* in marine deposits, while *Taenidium* was associated with root traces in both marine and terrestrial settings. In their study, vertical or inclined *Taenidium* burrows were related to terrestrial bioturbation, while horizontal burrows could be produced by marine invertebrates during the evolution of a shallowing-upward sequence.

CONCLUSIONS

- We suggest that the uppermost Devět Křížů Sandstone was deposited in a shallow-marine environment during the middle or early late Cenomanian, before the main phase of the late Cenomanian–early Turonian transgression phase.
- The results of our study exclude the possibility of association these deposits with the continental Triassic Bohdašín Formation.
- Apart from the exceptional palaeo-topographic and basin conditions that enabled this system to appear and be preserved, these deposits can be treated as an 'initial phase of transgression – precursor' at the beginning of the Late Cretaceous transgression in this part of the Sudetes.
- The sedimentological and biogenic features of the oldest Upper Cretaceous deposits (middle/early late Cenomanian) preserved in the Devět Křížů Sandstone profile in Krákorka, in light of the current knowledge about Recent subfossil and fossil spit bar deposits, allows us to suggest that the Krákorka deposits are indeed a fossil spit bar deposit.
- On the basis of palaeotransport landward directions we postulate a model of a recurved (hacked) spit (after King and Mc Cuulagh 1971).
- The spatial arrangement of facies, including the presence of sharp-edged intraclasts distributed at bedding surfaces and/or reactivation surfaces showing pseudoimbrication, as well as the presence of clay covers suggesting deposition from suspension and sedimentary structures (e.g., wave current ripples, through cross-stratification) indicating unidirectional transport, clearly support this premise.
- Moreover, the cyclic nature of sedimentation, alternating accumulation and erosional conditions, and environmental changes from shallow to slightly deeper marine (up to several metres), lower to high energy, and terrestrial to marine are suggestive of a spit bar setting.
- The studied sandstones contain root casts and rhizocretions, and may be regarded as a paleosol (? mangrove in origin) with initial soil development.
- The rhizolith-bearing horizon is moderate-to-highly bioturbated by cf. *Taenidium* isp., *Thalassinoides paradoxicus*, *T. suevicus*, cf. *Thalassinoides* isp. and some unrecognizable traces.
- Ichnological analysis captures the presence of two fossil suites, the *Thalassinoides* suite constructed by marine invertebrates and the cf. *Taenidium* suite produced by terrestrial tracemakers.
- The cf. *Taenidium* ichnofabric typical of the *Scoyenia* ichnofacies was reported in this locality for the first time. Bioturbation by terrestrial tracemakers, such as beetle larvae or cicada nymphs, occurred during periodic emergence of the spit bar.
- The *Thalassinoides* assemblage is characteristic of the allogenic expression of the *Glossifungites* ichnofacies, which indicates transgressional surfaces (firmgrounds), demarcating a depositional hiatus and erosional discontinuities. *Thalassinoides* bioturbation might have occurred during the late Cenomanian transgression, after prolonged emergence.

Acknowledgements

The authors would like to thank Diego Luciano Nascimento from Unisinos University (São Lepoldo, Brazil) and Adriano Santos Mineiro from the University of Brasília (Brasilía, Brazil) for insights and suggestions concerning the studied trace fossils. The authors are grateful to Huriye Demircan (Ankara, Turkey) and an anonymous reviewer for their comments, which considerably improved the final version of this manuscript. The authors also greatly appreciate the editoral support of Anna Żylińska.

REFERENCES

Abdel-Fattah, Z.A. and Gingras, M.K. 2020. Origin of compound biogenic sedimentary structures in Eocene strata of Wadi El-Hitan iniversal heritage area, Fayum, Egypt: Mangrove roots or not? *Palaeogeography, Palaeoclimatology, Palaeoecology*, **560**, 110048.

Abdel-Fattah, Z.A., Gingras, M.K., Caldwell, M.W. and Pemberton, S.G. 2010. Sedimentary environments and depositional characteristics of the Middle to Upper Eocene whale-bearing succession in the Fayum Depression, Egypt. *Sedimentology*, **57**, 446–476.

Abdel-Fattah, Z.A., Gingras, M.K., Caldwell, M.W., Pemberton, S.G. and MacEachern, J.A. 2016. The *Glossifungites* Ichnofacies and Sequence Stratigraphic Analysis: A Case Study from Middle to Upper Eocene Successions in Fayum, Egypt. *Ichnos*, **23**, 157–179.

Aleksandrowski, P., Śliwiński, W. and Wojewoda, J. 1986. Frontally and surficially fluidized slump to debris flow sheets in an alluvial sequence, Lower Permian, Intrasudetic Basin. In: Teisseyre A.K. (Ed.), IAS 7th European Regional Meeting, Excursion Guidebook, Kraków-Poland. Ossolineum, Wroclaw. Excursion A-1, 9–29.

Allard, J., Bertin, X., Chaumillon, E. and Pouget, F. 2008. Sand spit rhythmic development: A potential record of wave climate variations? Arçay Spit, western coast of France. *Marine Geology*, **253**, 107–131.

Ashton, A.D., Murray, A.B. and Littlewood, R. 2007. The Response of Spit Shapes to Wave-Angle Climates. In: Kraus, N.C. and Rosati, J.D. (Eds), Coastal sediments '07 – Proceedings of the 6th International Symposium on Coastal Engineering and Science of Coastal Sediment Processes, May 13–17, 2007, 351–363. American Society of Civil Engineers (ASCE); New Orleans, Louisiana, USA.

Averianov, A. and Ekrt, B. 2015. *Cretornis hlavaci* Frič, 1881 from the Upper Cretaceous of Czech Republic (Pterosauria, Azhdarchoidea). *Cretaceous Research*, **55**, 164–175.

Badawy, H.S. 2018. Termite nests, rhizoliths and pedotypes of the Oligocene fluviomarine rock sequence in northern Egypt: Proxies for Tethyan tropical palaeoclimate. *Palaeogeography, Palaeoclimatology, Palaeoecology*, **492**, 161–176.

Basyuni, M., Oku, H., Baba, S., Tokara, K. and Iwasaki, H. 2007. Isoprenoids of Okinawan mangroves as Lipid Input into Estuarine Ecosystem. *Journal of Oceanography*, **63**, 601–608.

Bengtson, S., Rasmussen, B., Zi, J.-W., Fletcher, I.R., Gehling, J.G. and Runnegar, B. 2021. Eocene animal trace fopssils in 1.7.-billion-year-old metaquartzites. *The Proceedings of the National Academy of Sciences PNAS*, **118**, 40 e2105707118.

Beni, A.N., Lahijani, H., Moussavi Harami, R., Leroy, S.A.G., Shah-Hosseini, M., Kabiri, K. and Tavakoli, V. 2013. Development of spit–lagoon complexes in response to Little Ice Age rapid sea-level changes in the central Guilan coast, South Caspian Sea, Iran. *Geomorphology*, **187**, 11–26.

Berry, M.E. and Staub, J.R. 1993. Root traces and the identification of paleosols. *INQUA Paleopedology Comission Newsletter*, **9**, 11–13.

Bertling, M., Braady, S., Bromley, R.G., Demathieu, G.R., Genise, J., Mikuláš, R., Nielsen, J.K., Nielsen, K.S.S., Rindsberg, A.K., Schlirf, M. and Uchman, A. 2006. Names for trace fossils: A uniform approach. *Lethaia*, **39**, 265–286.

Bertling, M., Buatois, L.A., Knaust, D., Laing, B., Mángano, M.G., Meyer, N., Mikuláš, R., Minter, N.J., Neumann, C., Rindsberg, A.K., Uchman, A. and Wisshak, M. 2022. Names for trace fossils 2.0: theory and practice in ichnotaxonomy. *Lethaia Review*, **55**, 1–19.

Bhattacharya, B., Banerjee, S. and Bandyopadhyay, S. 2016. *Glossifungites* ichnofabric signifying Crustacean colonization in early Permian barakar Formation, Talchir Coal basin, India. *Current Science*, **110**, 86–91.

Billy, J., Robin, N., J. Hein, C.J., Certain, R., and FitzGerald, D.M. 2014. Internal architecture of mixed sand-and-gravel beach ridges: Miquelon-Langlade Barrier, NW Atlantic. *Marine Geology*, **357**, 53–71.

Boer, P. de and Carr, A.P. 1969. Early Maps as Historical Evidence for Coastal Change. *The Geographical Journal*, **135**, 17–39.

Bojanowski, M.J., Jaroszewicz, E., Kosir, A., Łoziński, M., Marynowski, L., Wysocka, A. and Derkowski, A. 2016. Root-related rhodochrosite and concretionary siderite formation in oxygen-deficient conditions induced by a ground-water table rise. *Sedimentology*, **63**, 523–551.

Boyd, C. and McIlroy, D. 2017. Three-dimensional morphology of *Beaconites capronus* from Northeast England. *Ichnos*, **24**, 250–258.

Bradshaw, M. 1981. Paleoenvironmental interpretation and systematics of Devonian trace fossils from the Taylor Group (lower Beacon Supergroup), Antarctica. *New Zealand Journal of Geology and Geophysics*, **24**, 615–652.

Bromley, R.G. 1996. Trace Fossils. Biology. Taphonomy and Applications, 378 pp. Chapman and Hall; London.

Bromley, R.G. and Ekdale, A.A. 1986. Composite ichnofabrics and tiering of burrows. *Geological Magazine*, **123**, 59–65.

Buynevich, I.V., Bitinas, A. and Pupienis, D. 2007. Lithological anomalies in a relict coastal dune: Geophysical and paleoenvironmental markers. *Geophysical Research Letters*, **34**, L90707.

Čech, S. 2011. Palaeogeography and stratigraphy of the Bohemian Cretaceous Basin (Czech Republic) – an overview. *Geologické výzkumy na Moravé a ve Slezsku*, **2011** (1), 18–21.

Čech, S., Prouza, V., Mikuláš, R., Souček, M., Stárková, M., Rapprich, V. and Gürtlerová, P. 2018. Napříč Broumovským výběžkem. Česká geologická společnost. Exkurze Ceské geologické společnosti, 44. *ISBN 978-80-87487-22-8.*

Chakraborty, A., Hasiotis, S.T., Ghosh, B. and Bhattacharya, H.N. 2013. Fluvial trace fossils in the Middle Siwalik (Sarmatian–Pontian) of Darjeeling Himalayas, India. *Journal of Earth System Science*, **122**, 1023–1033.

Christiansen, Ch., Aagaard, T., Bartholdy, J., Christiansen, M., Nielsen, J., Nielsen, N., Pedersen, J.B.T. and Vinther, N. 2004. Total sediment budget of a transgressive barrier-spit, Skallingen, SW Denmark: A review. *Geografisk Tidsskrift-Danish Journal of Geography*, **104**, 107–126.

Chrząstek, A. and Wojewoda, J. 2022. *Rosselia* – a trace fossil indicator of beach-shoreface sedimentary settings in both transgressive and regressive sedimentary sequences of the Intra-Sudetic Basin. In: Jagt, J.W.M., Jagt-Yazykova, E., Walaszczyk, I. and Żylińska, A. (Eds), 11th International Cretaceous Symposium Warsaw, Poland, 2002, Abstract Volume, 138–139.

Clemmensen, L.B., Bendixen, M., Hede, M.U., Kroon, A., Nielsen, L. and Murray, A.S. 2014. Morphological records of storm floods exemplified by the impact of the 1872 Baltic storm on a sandy spit system in south-eastern Denmark. *Earth Surface Processes and Landforms*, **39**, 499–508.

Costas, S. and Fitzgerald, D. 2011. Sedimentary architecture of a spit-end (Salisbury Beach, Massachusetts): The imprints of sea-level rise and inlet dynamics. *Marine Geology*, **284**, 203–216.

Craig, M.S., Jol, H.M., Teitler, L. and Warnke, D.A. 2012. Geophysical surveys of a pluvial lake barrier deposit, Beatty Junction, Death Valley, California, USA. *Sedimentary Geology*, **269–270**, 28–36.

D'Alessandro, A. and Bromley, R.G. 1987. Meniscate trace fossils and the *Muensteria–Taenidium* problem. *Palaeontology*, **30**, 743–763.

D'Alessandro, A., Loiacono, F. and Bromley, R.G. 1993. Marine and nonmarine trace fossils and plant roots in a regressional setting (Pleistocene, Italy). *Rivista Italiana di Paleontologia e Stratigrafia*, **98**, 495–522.

Daly, J., McGeary, S. and Krantz, D.E. 2002. Ground-penetrating radar investigation of a late Holocene spit complex: Cape Henlopen, Delaware. *Journal of Coastal Research*, **18**, 274– 286.

Dorador, J. and Rodríguez-Tovar, F.J. 2014. Quantitative estimation of bioturbation based on digital image analysis. *Marine Geology*, **349**, 55–60.

Dreyer, T., Whitaker, M., Dexter, J., Flesche, H. and Larsen, E. 2005. From spit system to tide-dominated delta: integrated reservoir model of the Upper Jurassic Sognefjord Formation on the Troll West Field. In: Dore, A.G. and Vining, B.A. (Eds), Petroleum Geology: North-West Europe and Global Perspectives, Proceedings of the 6th Petroleum Geology Conference, 423–448. Geological Society; London.

Droser, M.L. and Bottjer, D.J. 1986. A semiquantitative field classification of ichnofabric. *Journal of Sedimentary Petrology*, **56**, 558–559.

Ehrenberg, K. 1944. Ergänzende Bemerkungen zu den seinerzeit aus dem Miozän von Burgschleinitz beschriebenen Gangkernen und Bauten dekapoder Krebse. *Paläontologische Zeitschrift*, **23**, 345–359.

Einsele, G., Ricken, W. and Seilacher, A. 1991. Cycles and events in stratigraphy, 955 pp. Springer-Verlag; Berlin, Heidelberg, New York.

Ekdale, A.A. and Bromley, R.G. 2003. Paleoethologic interpretation of complex *Thalassinoides* in shallow-marine limestones, Lower Ordovician, southern Sweden. *Palaeogeography, Palaeoclimatology, Palaeoecology*, **192**, 221–227.

Erbacher, J., Bornemann, A., Petrizzo, M.R. and Huck, S. 2020. Chemiostratigraphy and stratigraphic distribution of keeled planktonic foraminifera in the Cenomanian of the North German Basin. *Zeitschrift der Deutschen Gesellschaft für Geowissenschaften*, **171**, 149–161.

Esperante, R., Rodríguez-Tovar, F.J. and Nalin, R. 2021. Rhizoliths in lower Pliocene alluvial fan deposits of the Sorbas Basin (Almería, SE Spain). *Palaeogeography, Palaeoclimatology, Palaeoecology*, **567**, 110281.

Evans, O.F. 1942. The origin of spits, bars, and related structures. *The Journal of Geology*, **50**, 846–865.

Fatka, O., Budil, P. and Mikuláš, R. 2022. Healed injury in a nektobenthic trilobite: "*Octopus*-like" predatory style in Middle Ordovician? *Geologia Croatica*, **75**, 189–198.

Flemming, B. and Martin, C.K. 2021. Sedimentology of a coastal shelf sector characterised by multiple bedload boundaries: Plettenberg Bay, inner Agulhas Bank, South Africa. *Geo-Marine Letters*, **41**, 32.

Foster, C., Savrda, C.E., Demetz, E. and Sandlin, W. 2020. Firmground crustacean burrow systems (*Glossifungites* ichnofacies) in marine shelf deposits, Paleocene Clayton Formation, Alabama, USA. *Lethaia*, **53**, 500–514.

Fruergaard, M., Tessier, B., Poirier, C., Mouazé, D., Weill, P., Noël, S., Bristow, C. and Bristow, C. 2020. Depositional controls on a hypertidal barrier-spit system architecture and evolution, Pointe du Banc spit, north-western France. Depositional controls on a hypertidal barrier-spit system architecture and evolution, Pointe du Banc spit, north-western France. *Sedimentology*, **67**, 502–533.

Fürsich, F.T. and Mayr, H. 1981. Non-marine *Rhizocorallium* (trace fossil) from the Upper Freshwater Molasse (Upper Miocene) of southern Germany. *Neues Jahrbuch für Geologie und Paläontologie, Monatshefte*, **6**, 321–333.

Fürsich, F.T., Uchman, A., Alberti, M. and Pandey, D.K. 2018. Trace fossils of an amalgamated storm-bed succession from the Jurassic of the Kachchh Basin, India: The significance of time-averaging in ichnology. *Journal of Palaeogeography*, **7**, 14–31.

Genise, J.F. 2016. Ichnoentomology. Insect traces in soils and paleosols, 695 pp. Springer Cham.

Genise, J.F. 2019. Ichnoentomology: insect traces in soils, paleosols and other substrates. *Geology Today*, **35**, 29–38.

Genise, J.F., Alonso-Zarza, A.M., Krause, J.M., Sánchez, M.V., Sarzetti, L., Farina, J.L., González, M.G., Cosarinsky, M. and Bellosi, E.S. 2010. Rhizolith balls from the Lower Cretaceous of Patagonia: Just roots or the oldest evidence of insect agriculture? *Palaeogeography, Palaeoeclimatology, Palaeoecology*, **287**, 128–142.

Genise, J.F., Bellosi, E.S. and Gonzalez, M.G. 2004. An approach to the description and interpretation of ichnofabrics in paleosols. In: McIlroy, D. (Ed.), *The Application of Ichnology to Palaeoenvironmental and Stratigraphic Analysis*, **228**, 355–382.

Gillette, L., Pemberton, S.G. and Sarjeant, W.A.S. 2003. A Late Triassic invetebrate ichnofauna from Ghost Ranch, New Mexico. *Ichnos*, **10**, 141–151.

Gingras, M.K., Pemberton, S.G., Dashtgard, S. and Dafoe, L. 2008. How fast do marine invertebrates burrow? *Palaeogeography, Palaeoclimatology, Palaeoecology*, **270**, 280–286.

Gingras, M.K., Räsänen, M.E., Pemberton, S.G. and Romero, L.A. 2002. Ichnology and sedimentology reveal depositional characteristics of bay-margin parasequence in the Miocene Amazonian Foreland Basin. *Journal of Sedimentary Research*, **72**, 871–883.

Gowland, S., Taylor, A.M. and Martinius, A.W. 2018. Integrated sedimentology and ichnology of Late Jurassic fluvial point-bars – facies architecture and colonization styles (Lourinhã Formation, Lusitanian basin, Western Portugal). *Sedimentology*, **65**, 400–430.

Gregory, M.R., Martin, A.J. and Campbell, K.A. 2004. Compound trace fossils formed by plant and animal interactions: Quaternary of northern New Zealand and Sapelo Island, Georgia (USA). *Fossils and Strata*, **51**, 88–105.

Gupta, E. and Rajani, M.B. 2020. Historical coastal maps: importance and challenges in their use in studying coastal geomorphology. *Journal of Coastal Conservation*, **24**, 24.

Heer, O., von 1877. Flora fossils Helvetiae. Die Vorweltliche Flora des Schweiz, 182 pp. J. Wuster and Co.; Zurich.

Hejl, E., Heberer, B., Salcher, B., Sekyra, G., Van den haute, P. and Leichmann, J. 2023. Thermochronological constraints on the post-Variscan exhumation history of the southeastern Bohemian Massif (Waldviertel and Weinsberg Forest, Austria): palaeogeographic and geomorphologic implications. *International Journal of Earth Sciences*, **112**, 1203–1226.

Hiroki, Y. and Masuda, F. 2000. Gravelly spit deposits in a transgressive systems tract: the Pleistocene Higashikanbe Gravel, central Japan. *Sedimentology*, **47**, 135–149.

Holub, V. 1966. Geologické poměry Vychodního Podkrkonoši. Unpublished report, Charles University. Geofond ČR (National Centre for Applied Geosciences Information and Documentation); Praha.

Holub, V. 1972. Permian of the Bohemian Massif. In: Falke, H. (Ed.), Rotliegendes Essays on European Lower Permian, 137–188. E.J. Brill; Holland.

Howard, J.D. and Frey, R.W. 1984. Characteristic trace fossils in nearshore to offshore sequences, Upper Cretaceous of east-central Utah. *Canadian Journal of Earth Sciences*, **21**, 200–219.

Hsieh, S., Łaska, W. and Uchman, A. 2023. Intermittent and temporally variable bioturbation by some terrestrial invertebrates: implications for ichnology. *The Science of Nature*, **110**, 11.

Hsieh, S. and Uchman, A. 2023. Spatially associated or composite life traces from Holocene paleosols and dune sands provide evidence for past biotic interactions. *The Science of Nature*, **110**, 9.

Janušaitė, R., Jarmalavičius, D., Jukna, L., Žilinskas, G. and Pupienis, D. 2022. Analysis of Interannual and Seasonal Nearshore Bar Behaviour Observed from Decadal Optical Satellite Data in the Curonian Spit, Baltic Sea. *Remote Sensing*, **14**, 3423

Janušaitė, R., Jarmalavičius, D., Pupienis, D., Žilinskas, G. and Jukna, L. 2023. Nearshore sandbar switching episodes and their relationship with coastal erosion at the Curonian Spit, Baltic Sea. *Oceanologia*, **65**, 71–85.

Jerzykiewicz, T. and Wojewoda, J. 1986. The Radków and Szczeliniec sandstones: An example of giant foresets on a tectonically controlled shelf of the Bohemian Cretaceous Basin (Central Europe). In: Knight, R.J. and McLean, J.R. (Eds), Shelf Sands and Sandstones. *Canadian Society of Petroleum Geologists,* **11**, 1–35.

Jewell, P.W. 2007. Morphology and paleoclimatic significance of Pleistocene Lake Bonneville spits. *Quaternary Research*, **68**, 421–430.

Johannessen, P.N. and Nielsen, L.H. 2006. Spit-systems – An overlooked target in hydrocarbon exploration: The Holocene to Recent Skagen Odde, Denmark. *GEUS Bulletin Geological Survey of Denmark and Greenland Bulletin*, **10**, 17–20.

Johannessen, P.N. and Nielsen, H.N. 2009. Spit-system facies model – can this be used to reinterpret some of the isolated shelf sandstone ridges in the Cretaceous Western Interior Seaway, USA? Abstract Book, AAPG Convention & Exhibition, 7 June–10 June, 2009, 108–109. American Association of Petroleum Geologists; Denver.

Jol, H.M., Lawton, D.C. and Smith, D.G. 2002. Ground penetrating radar: 2-D and 3-D subsurface imaging of a coastal barrier spit, Long Beach, WA, USA. *Geomorphology*, **53**, 165–181.

Keighley, D.G. and Pickerill, R.K. 1994. The ichnogenus *Beaconites* and its distinction from *Ancorichnus* and *Taenidium*. *Palaeontology*, **37**, 305–337.

Kennedy, W.J. 1967. Burrows and surface traces from the Lower Chalk of southern England. Bulletin of the British Museum (Natural History). *Geology*, **15**, 125–167.

King, C.A.M. and Mc Cullagh, M.J. 1971. A simulation model of a complex recurved spit. *Journal of Geology*, **79**, 22–37.

King, M.R., La Croix, A.D., Gates, T.A., Anderson, P.B. and Zanno, L.E. 2021. *Glossifungites gingrasi* n. isp., a probable subaqueous insect domicile from the Cretaceous Ferron Sandstone, Utah. *Journal of Paleontology*, **95**, 427–439.

Klappa, C.F. 1980. Rhizoliths in terrestrial carbonates classification, recognition, genesis and significance. *Sedimentology*, **27**, 613–629.

Klappa, C.F. 2006. Rhizoliths in terrestrial carbonates: Classification, recognition, genesis and significance. *Sedimentology*, **27**, 613–629.

Knaust, D. 2015. Trace fossils from the continental Upper Triassic Kagerod Formation of Bornholm, Denmark. *Annales Societatis Geologorum Poloniae*, **85**, 481–492.

Knaust, D. 2017. Atlas of trace fossils in Well Cores. Appearance, Taxonomy and Interpretation, 209 pp. Spinger.

Knaust, D. 2021a. *Balanoglossites*-burrowed firmgrounds – the most common ichnofabric on earth? *Earth-Science Reviews*, **220**, 103747.

Knaust, D. 2021b. The paradoxical ichnotaxonomy of *Thalassinoides paradoxicus*: a name of different meanings. *Paläontologische Zeitschrift*, **95**, 179–186.

Korneisel, D., Gallois, R.W., Duffin, C.J. and Benton, M.J. 2015. Latest Triassic marine sharks and bony fishes from a bone bed preserved in a burrow system, from Devon, UK. *Proceedings of the Geologists' Association*, **126**, 130–142.

Kraus, M.J. and Hasiotis, S.T. 2006. Significance of different modes of rhizolith preservation to interpreting paleoenvironmental and paleohydrologic settings: Examples from Paleogene paleosols, Bighorn Basin, Wyoming, U.S.A. *Journal of Sedimentary Research*, **76**, 633–646.

Krause, J.M., Bown, T.M., Bellosi, E.S. and Genise, J.F. 2008. Trace fossils of cicadas in the Cenozoic of Central Patagonia, Argentina. *Palaeontology*, **51**, 405–418.

Krist, F. and Schaetzl, R.J. 2001. Paleowind (11,000 BP) directions derived from lake spits in Northern Michigan. *Geomorphology*, **38**, 1–18.

Leszczyński, S. and Nemec, W. 2015. Dynamic stratigraphy of composite peripheral unconformity in a foredeep basin. *Sedimentology*, **62**, 645–680.

Lindhorst, S., Betzler, C. and Hass, H.C. 2008. The sedimentary architecture of a Holocene barrier spit (Sylt, German Bight): swash-bar accretion and storm erosion. *Sedimentary Geology*, **206**, 1–16.

Lindhorst, S., Lampart, J., Hass, H.C. and Betzler, C. 2010. Anatomy and sedimentary model of a hooked spit (Sylt, southern North Sea). *Sedimentology*, **57**, 935–955.

Lobo, F.J., Fernandez-Salas, L.M., Hernandez-Molina, F.J., Gonzalez, R., Dias, J.M.A., Díaz del Río, V. and Somoza, L. 2005, Holocene highstand deposits in the Gulf of Cadiz, SW Iberian Peninsula: a high-resolution record of hierarchical environmental changes. *Marine Geology*, **219**, 109–131.

Lobo, F.J., González, R., Dias, J.M.A., Hernández-Molina, F.J., Fernández-Salas, L.M., Díaz del Río, V. and Somoza, L. 2003. Onshore-offshore comparison of late Holocene highstand deposits in the Gulf of Cadiz margin (SW Iberian Peninsula): a record of high-frequency environmental fluctuations. In: Mastronuzzi, G. and Sanso, P. (Eds), Field Guide, Quaternary coastal morphology and sea level changes. Final Conference Project IGCP 437 Coastal Environmental Change During Sea-Level Highstands: A Global Synthesis with implications for management of future coastal change. Otranto/Taranto–Puglia (Italy) 22–28 September 2003. Abstract Book, 149–152.

Lopez, E.D. 2022. An analog for large-scale lacustrine deposits: 3D characterization of a Pleistocene Lake Bonneville spit. Unpublished PhD Thesis, 53 pp. Brigham Young University, Provo UT.

MacEachern, J. and Bann, K.L. 2020. The *Phycosiphon* ichnofacies and the *Rosselia* ichnofacies: two new ichnofacies for marine deltaic environments. *Journal of Sedimentary Research*, **90**, 855–886.

MacEachern, J.A., Bann, K.L., Gingras, M.K., Zonneveld, J.-P., Dashtgard, S.E. and Pemberton, S.G. 2012. The ichnofacies paradigm. In: Knaust, D. and Bromley, R.G. (Eds), Trace fossils as indicators of sedimentary environments. *Developments in Sedimentology*, **64**, 103–138.

MacEachern, J.A., Pemberton, S.G., Gingras, M.K. and Bann, K.L. 2007. The ichnofacies paradigm: A fifty-year retrospective. In: Miller III, W. (Ed.), Trace fossils. Concepts, Problems, Prospects, 52–77. Elsevier.

MacEachern, J.A., Raychaudhuri, I. and Pemberton, S.G. 1992. Stratigraphic applications of the *Glossifungites* ichnofacies: Delineating discontinuities in the rock record. In: Pemberton, S.G. (Ed.), Applications of Ichnology to Petroleum Explorations, A Core Workshop. *SEPM Society for Sedimentary Geology*, **17**, 169–199.

Mader, D. 1982. Aeolian sands in continental red beds of the Middle Buntsandstein (Lower Triassic) at the western margin of the German Basin. *Sedimentary Geology*, **31**, 191–230.

Mader, D. 1983. Aeolian sands terminating an evolution of fluvial depositional environment in Middle Buntsandstein of the Eifel, Federal Republic Germany. In: Brookfield, M.E. and Ahlbrandt, T.S. (Eds), Eolian Sediments and Processes. *Developments in Sedimentology*, **38**, 583–612.

Mader, D. 1990. Palaecology of the flora in Buntsandstein and Keuper in the Triassic of Middle Europe. In: Fischer, G. (Ed.), Buntsandstein, vol. 1, 936 pp. Springer Verlag; Stuttgart, New York.

Mader, D. 1992. Bohdašín Formation (Buntsandstein). In: Mader, D. (Ed.), Evolution of palaeoecology and palaeoenvironments of Permian and Triassic fluvial basins in Europe, vol. 1, 501–555. Gustav Fischer-Verlag; Stuttgart.

Madzia, D. 2014. The first non-avian theropod from the Czech Republic. *Acta Palaeontologica Polonica*, **59**, 855–862.

Mángano, M.G. and Buatois, L.A. 2016. The Cambrian explosion. In: Mángano, M.G. and Buatois, L.A. (Eds), The trace-fossil record of major evolutionary events, vol. 1, Precambrian and Paleozoic. *Topics in Geobiology*, **39**, 71–126.

Marchetti, L., Collareta, A., Belvedere, M. and Leonardi, G. 2021. Ichnotaxonomy, biostratigraphy and palaeoecology of the Monti Pisani tetrapod ichnoassociation (Tuscany, Italy) and new insights on Middle Triassic Dinosauromorpha. *Palaeogeography, Palaeoclimatology, Palaeoecology*, **567**, 110235.

Martínek, K. and Štolfová, K. 2009. Provenance study of Permian non-marine sandstones and conglomerates of the Krkonoše Piedmont Basin (Czech Republic): exotic marine limestone pebbles, heavy minerals and garnet composition. *Bulletin of Geoscience*, **84**, 555–568.

Meistrell, F.J. 1972. The spit-platform concept: laboratory observation of spit development. In: Schwartz, M.L. (Ed.), Spits and Bars, 224–284. Dowden, Hutchinson and Ross; Stroudsburg, Pennsylvania.

Mencl, V., Bureš, J. and Sakala, J. 2013. Summary of occurrence and taxonomy of silicified *Agathoxylon*-type of wood on Late Paleozoic basins of the Czech Republic. *Folia*, **47**, 14–26.

Merletti, G.D., Steel, R.J., Olariu, C., Melick, J.J., Armitage, P.J. and Shabro, V. 2018. The last big marine transgression of the Western Interior Seaway: Almond Formation development from barrier spits across south Wyoming. *Marine and Petroleum Geology*, **98**, 763–782.

Mikuláš, R. 2019. Stop 2. Červeny Kostelec, U Devíti Křížů (also Krákorka) Quarry. In: Kočová Veselská, M., Adamovič, J., Kernhoff, M., Rifl, M., Samánek, J. and Mikuláš, R. (Eds), 15th International Ichnofabric Workshop, Prague, Czechia, April 27th–May 3rd, 2019, Program, Abstracts, Field Guidebook, 84–86. The Czech Academy of Sciences, Institute of Geology; Prague.

Mikuláš, R., Němečková, M. and Adamovič, J. 2002. Bioerosion and bioturbation of a weathered metavolcanic rock (Cretaceous, Czech Republic). *Acta Geologica Hispanica*, **37**, 21–27.

Mikuláš, R., Plička, M. and Skalický, J. 1991. A find of mud

scrolls in Lower Triassic sandstone at the locality Devět Křížů (NE Bohemia). *Věstnik Českého Geologického Ŭstavu*, **66**, 247–249. [In Czech with English summary]

Mikuláš, R. and Prouza, V. 1999. The Cretaceous biogenic structures created in Triassic sandstones (Devět křížů at Červený Kostelec, Bohemia, Czech Republic). *Věstnik Českého Geologického Ŭstavu*, **74**, 335–342.

Miller, M.F. and Smail, S.E. 1997. A semiquantitative field method for evaluating bioturbation on bedding planes. *Palaios*, **12**, 391–396.

Mineiro, A.S. and Santucci, R.M. 2018. Ichnofabrics and ichnofossils from the continental deposits of the Serra da Galga Member, Marília Formation, Bauru Group (Upper Cretaceous), Uberaba, Minas Gerais, Brazil. *Journal of South American Earth Sciences*, **86**, 287–300.

Mineiro, A.S., Santucci, R.M., Rocha, D.M.S. de, Andrade, M.B. de and Nava, W.R. 2017. Invertebrate ichnofossils and rhizoliths associated with rhizomorphs from the Marilía Formation (Echaporã Member), Bauru Group, Upper Cretaceous, Brazil. *Journal of South American Earth Sciences*, **80**, 529–540.

Mroczkowski, J. and Mader, D. 1985. Sandy inland braidplain deposition with local aeolian sedimentation in the lower and middle parts of the Buntsandstein and sandy coastal braidplain deposition in the top Zechstein in the Sudetes (Lower Silesia, Poland). *Lecture Notes in Earth Sciences*, **4**, 165–195.

Myrow, P.M. 1995. *Thalassinoides* and the enigma of Early Palaeozoic open-framework burrow systems. *Palaios*, **10**, 58–74.

Myrow, P.M. and Southard, J.B. 1996. Tempestite deposition. *Journal of Sedimentary Research*, **66**, 875–887.

Nádaskay, R. 2021. Mid-Cretaceous transgressions on the northern edge of Prague. Guidebook to field trip FT12 (19 June 2021). 35th IAS Meeting of Sedimentology, June 21–25, 2021. Prague, Czech Republic.

Nádaskay, R., Žák, J., Sláma, J., Sidorinová, T. and Valečka, J. 2019. Deciphering the Late Paleozoic to Mesozoic tectonosedimentary evolution of the northern Bohemian Massif from detrital zircon geochronology and heavy mineral provenance. *International Journal of Earth Sciences*, **108**, 2653–2681.

Nascimento, D.L., Batezelli, A. and Ladeira, F.S.B. 2019. The paleoecological and paleoenvironmental importance of root traces: Plant distribution and topographic significance of root patterns in Upper Cretaceous paleosols. *Catena*, **172**, 789–806.

Nascimento, D.L., Netto, R.G., Batezelli, A., Ladeira, F.S.B. and Sedorko, D. 2023. *Taenidium barretti* ichnofabric and rainfall seasonality: Insights into dryland suites of *Scoyenia* ichnofacies. *Journal of Palaeogeography*, **12**, 28–49.

Neal, A. 2004. Ground-penetrating radar and its use in sedimentology: principles, problems and progres. *Earth-Science Reviews*, **66**, 261–330.

Nehyba, S. and Roetzel, R. 2021. Coastal sandy spit deposits (Lower Burdigalian/Eggenburgian) in the Alpine-Carpathian Foredeep of Lower Austria. *Geological Quarterly*, **65**, 50.

Nielsen, L.H. and Johannessen, P.N. 2009. Facies architecture and depositional processes of the Holocene–Recent accretionary forced regressive Skagen spit system, Denmark. *Sedimentology*, **56**, 935–968.

Nielsen, L.H., Johannessen, P.N. and Surlyk, F. 1988. A Late Pleistocene coarse-grained spit-platform sequence in northern Jylland, Denmark. *Sedimentology*, **35**, 915–937.

Novak, B. and Pedersen, G.K. 2000. Sedimentology, seismic facies and stratigraphy of a Holocene spit-platform complex interpreted from high-resolution shallow seismics, Lysegrund, southern Kattegat, Denmark. *Marine Geology*, **162**, 317–335.

Ollerhead, J. and Davidson-Arnott, R.G.D. 1995. The evolution of Buctouche Spit, New Brunswick, Canada. *Marine Geology*, **124**, 215–236.

Opluštil, S., Schmitz, M., Kachlík, U. and Stamberg, S. 2016. Re-assessment of lithostratigraphy, biostratigraphy, and volcanic activity of the Late Paleozoic Intra-Sudetic, Krkonoše-Piedmont and Mnichovo-Hradište basins (Czech Republic) based on new U-Pb CA-ID-TIMS ages. *Bulletin of Geosciences*, **91**, 399–432.

Opluštil, S., Šimůnek, Z. and Mencl, V. 2022. Macroflora of the Krkonoše-Piedmont Basin (Pennsylvanian–early Permian); Bohemian Massif, Czech Republic. *Review of Palaeobotany and Palynology*, **303**, 104665.

Pancrazzi, L. 2022. Dynamique et structure interne de barrières littorales sablo-graveleuses en environnement hypertidal: approches expérimentale et in-situ. Unpublished Doctoral thesis, 216 pp. Normandie Université, Caen.

Pancrazzi, L., Weill, P., Tessier, B., Le Bot, S. and Benoit, L. 2022. Morphostratigraphy of an active mixed sand-gravel barrier spit (Baie de Somme, northern France). *Sedimentology*, **69**, 2753–2778.

Panin, N. and Overmars, W. 2012. The Danube delta evolution during the Holocene: reconstruction attempt using geomorphological and geological data, and some of the existing cartographic documents. *Geo-Eco-Marina*, **18**, 75–104.

Pellerin Le Bas, X, Levoy, F., Robin, N. and Anthony, E.J. 2022. The formation and morphodynamics of complex multi-hooked spits and the contribution of swash bars. *Earth Surface Processes and Landforms*, **47**, 159–178.

Pemberton, S.G. and Gingras, M.K. 2005. Classification and characterizations of biogenically enhanced permeability. *AAPG Bulletin*, **89**, 1493–1517.

Pemberton, S.G., MacEachern, J.A., Dashtgard, S.E., Bann, K.L., Gingras, M.K. and Zonneveld, J.-P. 2012. Shorefaces. In: Knaust, D. and Bromley, R.G. (Eds), Trace fossils as indicators of sedimentary environments. *Developments in Sedimentology*, **64**, 563–603.

Peterson, C.D., Williams, S.S., Cruikshank, K.M. and Dubè, J.R. 2011. Geoarchaeology of the Nehalem spit: Redistribution of beeswax galleon wreck debris by Cascadia earthquake

and tsunami (~A.D. 1700), Oregon, USA. *Geoarchaeology*, **26**, 219–244.

Pervesler, P. and Uchman, A. 2009. A new Y-shaped trace fossil attributed to upogebiid crustaceans from Early Pleistocene of Italy. *Acta Palaeontologica Polonica*, **54**, 135–142.

Plaziat, J.C. and Mahmoudi, M. 1990. The role of vegetation in Pleistocene eolianite sedimentation; an example from Eastern Tunisia. *Journal of African Earth Sciences*, **10**, 445–451.

Porrenga, D.H. 1967. Glauconite and chamosite as depth indicators in the marine environment. *Marine Geology*, **5**, 495–501.

Prouza, V. 1988. Geologická Mapa ÈSR. List 04-32 Broumov, 1:50 000. Ústřední Ústav Geologický; Praha.

Prouza, V. and Tasler, R. 1985. Přehledná geologická mapa podkrkonošské pánve. Ústřední Ustav Geologický; Praha.

Prouza, V., Tásler, R., Valin, F. and Vlastimil, H. 1985. Gravelly to sandy braidplain deposition in the Buntsandstein-facies Bohdašín Formation in norteastern Bohemia (Czechoslovakia). In: Mader, D. (Ed.), Aspects of fluvial sedimentation in the lower Triassic Buntsandstein of Europe. *Lecture Notes in Earth Sciences*, **4**, 397–410.

Rasmussen, E.S. and Dybkjær, K. 2005. Sequence stratigraphy of the Upper Oligocene–Lower Miocene of eastern Jylland, Denmark: role of structural relief and variable sediment supply in controlling sequence development. *Sedimentology*, **52**, 25–63.

Rasmussen, E.S., Dybkjær, K. and Piasecki, S. 2010. Lithostratigraphy of the upper Oligocene–Miocene succession in Denmark. *Bulletin of the Geological Society of Denmark*, **22**, 1–92.

Reimann, T., Lindhorst, S., Thomsen, K.J., Murray, A.S. and Frechen, M. 2012. OSL dating of mixed coastal sediment (Sylt, German Bight, North Sea). *Quaternary Geochronology*, **11**, 52–67.

Retallack, G.J. 1976. Triassic palaeosols in the upper Narrabeen Group of New South Wales. Part I: Features of the palaeosols. *Journal of the Geological Society of Australia*, **23**, 383–399.

Retallack, G.J. 1988. Field recognition of paleosols. *Geological Society of America, Special Papers*, **216**, 1–20.

Retallack, G.J. 2001. Soils of the Past: An Introduction to Paleopedology, 520 pp. Blackwell; Oxford.

Rieth, A. 1932. Neue Funde spongeliomorpher Fucoiden aus Jura Schwabens. *Geologische Paläontologische Abhandlungen, Neue Folge*, **19**, 257–294.

Robin, N., Levoy, F., Anthony, E.J. and Monfort, O. 2020. Sand spit dynamics in a large tidal-range environment: Insight from multiple LiDAR, UAV and hydrodynamic measurements on multiple spit hook development, breaching, reconstruction, and shoreline changes. *Earth Surface Processes and Landforms*, **45**, 2706–2726.

Rodríguez-Santalla, I., Gomez-Ortiz, D., Martín-Crespo, T., Sánchez-García, M.J., Montoya-Montes, I., Martín-Velázquez, S., Barrio, F., Serra, J., Ramírez-Cuesta, J.M. and Gracia, F.J. 2021. Study and evolution of the dune field of La Banya Spit in Ebro Delta (Spain) using LiDAR Data and GPR. *Remote Sensing*, **13**, 802.

Rodríguez-Santalla, I. and Somoza, L. 2018. The Ebro River delta. In: Morales, J.A. (Ed.), The Spanish Coastal Systems, 467–488. Springer Nature; Switzerland AG.

Rodríguez-Tovar, F.J., Alcála, L. and Cobos, A. 2016. *Taenidium* at the Lower Barremian El Hoyo dinosaur tracksite (Teruel, Spain): Assessing palaeoenvironmental conditions for the invertebrate community. *Cretaceous Research*, **65**, 48–58.

Rubio, B. and López-Pérez, A.E. 2024. Exploring the genesis of glaucony and verdine facies for paleoenvironmental interpretation: A review. *Sedimentary Geology*, **461**, 106579.

Salter, J.W. 1857. On annelide-burrows and surface-markings from the Cambrian rocks of the Longmynd. No 2. *Geological Society of London, Quarterly Journal*, **13**, 199–206.

Sarjeant, W.A.S. 1975. Plant trace fossils. In: Frey R.W. (Ed.), The Study of Trace Fossils, 163–179. New York; Springer Verlag.

Schaetzl, R.J., Krist Jr, F.J., Lewis, C.F.M., Luehmann, M.D. and Michalek, M.J. 2016. Spits formed in Glacial Lake Algonquin indicate strong easterly winds over the Laurentian Great Lakes during late Pleistocene. *Journal of Paleolimnology*, **55**, 49–65.

Sedorko, D., Alessandretti, L., Warren, L.V., Verde, M., Rangel, C.C., Ramos, K.S. and Netto, R.G. 2020. Trace fossils from the Upper Cretaceous Capacete Formation, Sanfranciscana Basin, Central Brazil. *Annales Societatis Gelogorum Poloniae*, **90**, 247–260.

Shan, X., Yu, X., Clift, P. D., Tan, C., Jin, L., Li, M. and Li, W. 2015. The Ground Penetrating Radar facies and architecture of a Paleo-spit from Huangqihai Lake, North China: Implications for genesis and evolution. *Sedimentary Geology*, **323**, 1–14.

Shaw, J., Wu, Y. and Potter, D.P. 2019. Distribution and morphology of inner-shelf sand bodies off southwest Newfoundland based on merged multibeam sonar and lidar data. *Canadian Journal of Earth Sciences*, **57**, 114–122.

Shawler, J.L., Hein, C.J., Obara, C.A., Robbins, M.G., Huot, M.G. and Fenster, M.S. 2021. The effect of coastal landform development on decadal-to millennialscale longshore sediment fluxes: Evidence from the Holocene evolution of the central mid-Atlantic coast, USA. *Quaternary Science Reviews*, **267**, 107096.

Shukla, S.B., Patidar, A.K. and Bhatt, N. 2008. Application of GPR in the study of shallow subsurface sedimentary architecture of Modwa spit, Gulf of Kachchh. *Journal of Earth System Science*, **117**, 33–40.

Simeoni, U., Fontolan, G., Tessari, U. and Corbau, C. 2007. Domains of spit evolution in the Goro area, Po Delta, Italy. *Geomorphology*, **86**, 332–348.

Šimůnek, T. 2019. Revision of the genus *Cordaites* UNGER from the Permian of the Intrasudetic Basin (Broumov Formation, Olivêtin Member, Czech Republic). *Geologia Croatica*, **72**, 163–172.

Śliwiński, W. 1984. Proposed revision of Chełmsko Śląskie Beds (Permian, Intra-Sudetic Basin. *Geologia Sudetica*, **18**, 167–174. [In Polish with English summary]

Smith, J.J., Hasiotis, S.T., Kraus, M.J. and Woody, D.T. 2008. *Naktodemasis bowni*: new ichnogenus and ichnospecies for adhesive meniscate burrows (AMB), and paleoenvironmental implications, Paleogene Willwood Formation, Bighorn Basin, Wyoming. *Journal of Paleontology*, **82**, 267–278.

Somoza, L. and Rodríguez-Santalla, I. 2014. Geology and geomorphological evolution of the Ebro River Delta. In: Gutiérrez, F. and Gutiérrez, M. (Eds), Landscapes and Landforms of Spain, World Geomorphological Landscapes, 213–227. Springer Science+Business Media; Dordrecht.

Spaggiari, R. and Bordy, E.M. 2023. Anatomy of a diamondiferous gravel barrier spit at the palaeo-Orange River mouth, south-western Namibia. *Sedimentology*, **70**, 1630–1654.

Špičaková, L., Uličný, D. and Svobodová, M. 2014. Phases of the mid-Cenomanian transgression recorded in a composite palaeovalley fill – the Horoušany quarry, Bohemian Cretaceous Basin. *Zeitschrift der Deutschen Gesellschaft für Geowissenschaften*, **165**, 581–619.

Srikanth, S., Lum, S.K.Y. and Chen, Z. 2015. Mangrove root: adaptations and ecological importance. *Trees*, **30**, 451–465.

Srivastava, J. and Prasad, V. 2019. Evolution and paleobiogeography of mangroves. *Marine Ecology*, **40**, e12571.

Tásler, R. 1995. Geological Map of the Czech Republic 1:50 000, Sheet Meziměstí 04-31. Czech Geological Survey, Prague, Czech Republic. [In Czech]

Taveneau, A., Almar, R., Bergsma, E., Sy, B.A., Ndour, A., Sadio, M. and Garlan, T. 2021. Observing and predicting coastal erosion at the Langue de Barbarie sand spit around Saint Louis (Senegal, West Africa) through satellite-derived Digital Elevation Model and shoreline. *Remote Sensing*, **13**, 2454.

Taylor, A.M. and Goldring, R. 1993. Description and analysis of bioturbation and ichnofabric. *Journal of the Geological Society*, **150**, 141–148.

Taylor, A., Goldring, R. and Gowland, S. 2003. Analysis and application of ichnofabrics. *Earth-Science Reviews*, **60**, 227–259.

Teisseyre, A.K. 1968. The Lower Carboniferous of the Intrasudetic Basin: a study in sedimentary petrology and basin analysis. *Geologia Sudetica*, **4**, 221–298.

Teisseyre, A.K. 1973. Carboniferous fans and fanglomerates in the Central Sudetes 1: Marginal faults, downfaulting and sedimentation. *Bulletin of the Polish Academy of Sciences, Earth Sciences*, **21**, 147–155.

Teisseyre, A.K. 1975. Sedimentology and palaeogeography of the Kulm alluvial fans in the western Intrasudetic Basin (Central Sudetes, SW Poland). *Geologia Sudetica*, **9**, 5–135.

Teisseyre, A.K. and Teisseyre, J. 1969. Faulting and sedimentation on the north-western margin of the Intrasudetic Basin. *Bulletin of the Polish Academy of Sciences, Earth Sciences*, **17**, 41–48.

Tiffany, M. R., Ping, W. and Jack, A.P. 2013. Storm-driven cyclic beach morphodynamics of a mixed sand and gravel beach along the Mid-Atlantic Coast, USA. *Marine Geology*, **346**, 403–421.

Tillmann, T. and Wunderlich, J. 2013. Barrier rollover and spit accretion due to the combined action of storm surge induced washover events and progradation: Insights from ground-penetrating radar surveys and sedimentological data. In: Conley, D.C., Masselink, G., Russell, P.E. and O'Hare, T.J. (Eds), Proceedings 12th International Coastal Symposium (Plymouth, England). *Journal of Coastal Research, Special Issue*, **65**, 600–605.

Tillmann, T. and Wunderlich, J. 2014. Barrier spit accretion model of Southern Sylt, German North Sea: Insights from ground-penetrating radar surveys and sedimentological data. *Zeitschrift für Geomorphologie*, **68**, 137–161.

Uchman, A., Dávid, Á. and Fodor, R. 2023. Clasts derived from rhizocretions in shallow-marine Miocene clastic deposits of northern Hungary: an example of zombie biogenic structures. *Geological Quarterly*, **67**, 4.

Uchman, A., Ślączka, A. and Renda, P. 2012. Probable root structures and associated trace fossils from the Lower Pleistocene calcarenites of Favignana Island, southern Italy: dilemmas of interpretation. *Geological Quarterly*, **56**, 745–756.

Uličný, D. 2001. Depositional systems and sequence stratigraphy of coarse-grained deltas in a shallow-marine, strike-slip setting: the Bohemian Cretaceous Basin, Czech Republic. *Sedimentology*, **48**, 599–628.

Uličný, D. 2004. A drying-upward aeolian system of the Bohdašín Formation (Early Triassic), Sudetes of NE Czech Republic: record of seasonality and long-term palaeoclimate change. *Sedimentary Geology*, **167**, 17–39.

Uličný, D., Špičáková, L. and Čech, S. 2003. Changes in depositional style of an intra-continental strike-slip basin in response to shifting activity of basement fault zones: Cenomanian of the Bohemian Cretaceous. Basin. *GeoLines*, **16**, 133–148.

Uličný, D., Špičáková, L., Grygar, R., Svobodová, M., Čech, S. and Laurin, J. 2009. Palaeodrainage systems at the basal unconformity of the Bohemian Cretaceous Basin: roles of inherited fault systems and basement lithology during the onset of basin filling. *Bulletin of Geosciences*, **84**, 577–610.

Valečka, J. 2019. Jurassic pebbles in the Cretaceous sandstones of the Bohemian Basin as a possible tool for reconstruction of the Late Jurassic and Late Cretaceous palaeogeography. *Volumina Jurassica*, **17**, 17–38.

Valín, F. 1964. Lithology of Triassic deposits in NE Czech Republic. *Véstník Českého Geologického Ústavu*, **39**, 459–462. [In Czech]

Vejbæk, O.V., Anderson, C., Dusa, M., Herngreen, W., Krabbe, H. and Leszczyński, K. 2010. Cretaceous. In: Doornenbal, H. and Stevenson, A. (Eds), Petroleum Geological Atlas of

the southern Permian Basin area, 195–209. EAGE Publications BV; Utrecht, Netherlands.

Vejlupek, M. 1983. Stratigraphic position of the Devět Křížů Sandstone. *Věstník Českého Geologického Ústavu*, **58**, 57–59. [In Czech]

Vejlupek, M. 1990. Geological Map of the Czech Republic 1:50 000, Sheet Náchod 04-33. Czech Geological Survey, Prague, Czech Republic. [In Czech]

Verde, M., Ubilla, M., Jiménez, J.J. and Genise, J.F. 2007. A new eartworm trace fossil from paleosols: Aestivation chambers from the Late Pleistocene Sopas Formation of Uruguay. *Palaeogeography, Palaeoclimatology, Palaeoecology*, **243**, 339–347.

Villegas-Martin, J., Netto, R.G. and Kern, H.P. 2020. Differences between autogenic and allogenic expressions of the *Glossifungites* Ichnofacies in estuarine and shoreface deposits from the Permian of the Paraná Basin, Brazil. *Geological Journal*, **55**, 6974–6988.

Voigt, S., Wagreich, M., Surlyk, F., Walaszczyk, I., Uličný, D., Čech, S., Voigt, T., Wiese, F., Wilmsen, M., Niebuhr, B., Reich, M., Funk, H., Michalík, J., Jagt, J.W.M., Felder, P.J. and Schulp, A.S. 2008. Chapter 15. Cretaceous, 923–997. In: McCann, T. (Ed.), The geology of Central Europe, Vol. 2. Mesozoic and Cenozoic. The Geological Society; London.

Voigt, T. 2009. Die Lausitz-Riesengebirgs-Antiklinalzone als kreidezeitliche Inversionsstruktur: Geologische Hinweise aus den umgebenden Kreidebecken. *Zeitschrift für geologische Wissenschaften*, **37**, 15–39.

Voigt, T., Kley, J. and Voigt, S. 2021. Dawn and dusk of Late Cretaceous basin inversion in central Europe. *Solid Earth*, **12**, 1443–1471.

Wilmsen, M., Niebuhr, B., Fengler, M., Püttmann, T. and Berensmeier, M. 2019. The Late Cretaceous transgression in the Saxonian Cretaceous Basin (Germany): old story, new data and novel findings. *Bulletin of Geosciences*, **94**, 71–100.

Wilmsen, M., Uličný, D. and Košťák, M. 2014. Cretaceous basins of Central Europe: deciphering effects of global and regional processes – a short introduction. *Zeitschrift der Deutschen Gesellschaft für Geowissenschaften*, **165**, 495–499.

Wojewoda, J. 1986. Fault scarp induced shelf sand bodies in Upper Cretaceous of the Intrasudetic Basin. In: Teisseyre, A.K. (Ed.), 7 JAS Regional Meeting Guidebook, Excursion A-T, 1–30. Ossolineum; Wrocław.

Wojewoda, J. 2007a. Neotectonic aspect of the Intrasudetic shear zone. *Acta Geodynamica et Geomaterialia*, **4** (148), 1–11.

Wojewoda, J. 2007b. Žďárky–Pstrążna Dome – dextral strike-slip fault related structure at the eastern termination of the Poříčí–Hronov Fault Zone (Sudetes, Góry Stołowe Mts.). In: Venera, Z. (Ed.), 5th Meeting of the Central European Tectonic Studies Group (CETEG'5), April 11–14.04.2007, Tepla, 93–96. Czech Geological Survey.

Wojewoda, J. 2007c. Palaeogeography and tectonic evolution of the Žernov–Náchod–Kudowa sedimentary area. In: Venera, Z. (Ed.), 5th Meeting of the Central European Tectonic Studies Group (CETEG'5), April 11–14.04.2007, Tepla, 96–98. Czech Geological Survey.

Wojewoda, J. 2008. Diffusional cells – an example of differentiated rheological reaction of granular sediment to seismic shock. *Przegląd Geologiczny*, **56**, 842–847. [In Polish with English abstract]

Wojewoda, J. 2009. Žďarky-Pstrążna Dome: a strike-slip fault-related structure at the eastern termination of the Poříčí-Hronov Fault Zone (Sudetes). *Acta Geodynamica et Geomaterialia*, **6** (3), 273–290.

Wojewoda, J., Chrząstek, A. and Sokalski, D. 2022. Late Cretaceous geodynamics in the Middle Sudetes area (sedimentary and ichnological record). In: Todes, J. and Walaszczyk, I. (Eds), Cretaceous of Poland and adjacent areas: field trip guides, 11th International Cretaceous Symposium, Warsaw, Poland, 2022, 191–241. Uniwersytet Warszawski; Warszawa.

Wojewoda, J. and Kowalski, A. 2016. Rola południowo-sudeckiej strefy ścinania w ewolucji Sudetów. In: Wyzwania Polskiej Geologii – 3. Polski Kongres Geologiczny. In: Wojewoda, J. and Kowalski, A. (Eds), Przewodnik do Wycieczek Kongresowych, wycieczka 2.3, 21–43, Polskie Towarzystwo Geologiczne; Wrocław.

Wojewoda, J., Rauch, M. and Kowalski, A. 2016. Synsedimentary seismotectonic features in Triassic and Cretaceous sediments of the Intrasudetic Basin (U Devěti křížů locality) – regional implications. *Geological Quarterly*, **60**, 355–364.

Woodward, S. 1830. A synoptic table of British organic remains, i–xiii, 1–50. Longman & John Stacy; London.

Zajíc, J. 1998. The first find of the dinosaurian footprint in the Czech Republic (the Krkonoše Piedmont Basin) and its stratigraphic significance. *Journal of the Czech Geological Society*, **43**, 273–276.

Zajíc, J. 2014. Permian fauna of the Krkonoše Piedmont Basin (Bohemian Massif, central Europe). *Acta Musei Nationalis Pragae*, **70**, 131–142.

Zhang, L.-J., Qi, Y.-A., Buatois, L.A., Mángano, M. G., Meng, Y. and Li, D. 2017. The impact of deep-tier burrow systems in sediment mixing and ecosystem engineering in early Cambrian carbonate settings. *Scientific Reports*, **7**, 45773.

Manuscript submitted: 31st August 2023
Revised version accepted: 24th May 2024